University of Stavanger

Faculty of Science and Technology

MASTER'S THESIS

Study program/ Specialization: Petroleum Engineering/ Drilling and Well Technology	Spring semester, 2014 Open
Writer: ***André Time***	…… (Writer's signature)
Faculty supervisor: Dan Sui External supervisor(s):	
Thesis title: ***Dual Gradient Drilling - Simulations during connection operations***	
Credits (ECTS): 30	
Key words: • Dual Gradient Drilling • Connection operations • Control theory	Pages: 63 + enclosure: 20 Stavanger, 14th of June, 2014

Acknowledgements

This report is the result of my master's thesis at the University of Stavanger, carried out during the spring of 2014.

I would like to thank my family and friends for their encouragement and support during my years as a student at UiS. I would also like to thank my supervisor Dan Sui for her support and guidance during my work with this thesis.

Abstract

As oilfields are ageing and depleting, operators are forced to start searching for oil in more hostile environments. These new environments can introduce new drilling challenges. Prospects like ultra deep water reservoirs and depleted offshore reservoirs are difficult to drill with conventional drilling. This has lead the industry to developing the Dual Gradient Drilling (DGD) system.

DGD is an unconventional drilling method and it is classified as a Managed Pressure Drilling (MPD) technique. By using fluids of varying density, DGD can provide the desired annular pressure profile in order to increase well performance, improve personnel safety and reduce Non Productive Time (NPT). Four major dual gradient drilling methods, along with the most important equipment, will be presented in this thesis.

The various MPD technologies tries to compensate for the pressure variations experienced in the wellbore during connections. These pressure variations can cause formation fracturing, lost circulation, stuck pipe and more. By utilizing the DGD system the pressure variation related to connection operations can be significantly reduced. Although this new technology has several advantages over conventional drilling, it also has its challenges.

To study the effects the DGD system has on downhole pressure during connection operations, the Kaasa model is used to simulate a DGD well and the results are compared to an MPD well.

Table of Contents

Nomenclature

Abbreviations

BHA	Bottomhole Assembly
BHP	Bottomhole Pressure
BOP	Blowout Preventer
CAPM	Continuous Annular Pressure Management
CML	Controlled Mud Level
DGD	Dual Gradient Driling
DSV	Drillstring Valve
ECD	Equivalent Circulating Density
IADC	International Association of Drilling Contractors
MPD	Managed Pressure Drilling
MRL	Mud Return Line
NPT	Non- Productive Time
RCD	Rotating Control Device
RDJ	Riser Dump Joint
RMR	Riserless Mud Recovery
ROP	Rate of Penetration
ROV	Remotely Operated Vehicle
SMD	Subsea Mudlift Drilling
SMO	Suction Module
SPM	Subsea Pump Module
SPU	Solids Processing Unit
SRD	Subsea Rotating Device
TD	Target Depth
TVD	True Vertical Depth

1 Dual Gradient Drilling

The International Association of Drilling Contractors (IADC) currently defines dual gradient as follows:

"*Two or more pressure gradients within selected well sections to manage the well pressure profile.*" (IADC, 2011)

The dual gradient drilling (DGD) technology has made it possible to drill in environments that no one thought possible just a few years ago. This technology is an unconventional drilling technology and is internationally regarded as important to enable drilling in depleted reservoirs and in deep waters. Dual gradient drilling relies on using fluids with different densities to create a pressure gradient which better suits the formation pressure profile. The DGD method can also eliminate the "pump and dump" practice where all mud returns are dumped on the seafloor. This reuse of mud allows for drilling with a more suitable mud instead of a cheap and disposable mud. It also opens the possibility for drilling in environmentally sensitive areas where a pump and dump operation would not be permitted. (Østvik, 2011) (Statoil, 2014)

In a well drilled with the DGD technology, the well pressure is the sum of two different fluid gradients, a riser fluid gradient, gas or liquid, and a drilling fluid gradient. The adjustment of the fluid level in the riser can ensure that the wellbore pressure is kept within the pore pressure and fracture pressure gradients through a longer depth interval compared to conventional drilling. This technique will effectively widen the drilling window and lower the risk of unexpected drilling problems. (Østvik, 2011) (Statoil, 2014) (Hsieh & Scott, 2012)

1.1 Background/History

In the early 1960s the drilling industry started developing an interest for a dual gradient drilling system. The goal of this new system would be to eliminate the need for a riser during drilling. Therefore, the concept was referred to as "Riserless Drilling". The technology at the time was not sufficient to develop this new system. The need for such a system was not too

great either. At the water depths they were planning to drill, the conventional riser-based technology proved adequate. (Smith K., Gault, Witt, & Weddle, 2001)

In the 1990s, several significant deepwater discoveries where made in the Gulf of Mexico and the need for a dual gradient drilling system arose again. The increase in lease sales for these deepwater blocks and the limited supply of deepwater drilling rigs motivated operators and contractors to develop a technology for shallow water drilling rigs to be used at deeper waters. It was evident that a dual gradient drilling system could be solution they were looking for. The advantages of this technology were well documented, but developing this challenging technology required a new way of thinking. (Haj, 2012) (Østvik, 2011)

Around 1996, four projects started developing the dual gradient drilling technology. Shell Oil Co.'s project, the Subsea Mudlift Drilling Joint Industry Project, the Deep Vision Project and Maurer Technology's Hollow Spheres Project were all developing technologies for use in water depths greater than 1500m. Five years later, in 2001, a dual gradient well was successfully drilled at 300m water depth in the Gulf of Mexico, a world first. Through close monitoring and thorough examination of test results, this first well showed that a real well could be drilled with the dual gradient drilling system. (Schubert, Juvkam-Wold, & Choe, 2006) (Østvik, 2011)

1.2 Breif overview of dual gradient drilling

Dual gradient drilling is classified as a managed pressure drilling (MPD) method and is an alternative to conventional drilling methods. The system is characterized by two or more pressure gradients used to manage the well pressure profile. Several dual gradient drilling systems has been developed. The various systems utilize either a subsea mudlift pump close to or on the seabed with a mud return line to transport mud and cuttings to the surface, or a subsea pump module and mud return line attached to a modified riser at a predetermined depth between surface and seabed. The dual gradient drilling system significantly increases the margin between the pore and fracture pressure gradients. (Haj, 2012) (Smith K., Gault, Witt, & Weddle, 2001) (Fossli & Sangesland, Controlled Mud-Cap Drilling for Subsea Applications: Well-Control Challenges in Deep Waters, 2006)

2 Dual gradient drilling methods

The International Association of Drilling Contractors' Dual Gradient Drilling Subcommittee recently classified dual gradient systems into two main categories. A DGD system installed prior to running the blowout preventer (BOP) is classified as a pre-BOP system while a DGD system installed after the BOP has been run is classified as a post-BOP system. The classification looks like this:

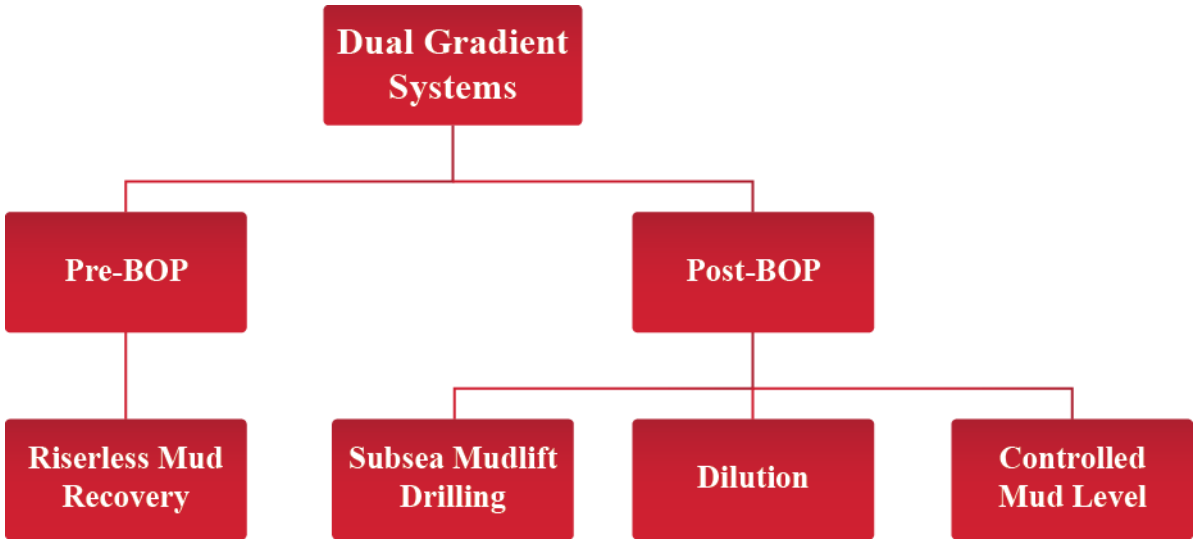

Figure 2-1. Dual Gradient Drilling classification

2.1 Pre-BOP

This subchapter will present an overview of the Pre-BOP classified DGD system called Riserless Mud Recovery.

2.1.1 Riserless Mud Recovery

When drilling the tophole intervals of deepwater wells with a conventional drilling method a riser is commonly not used. Cuttings and mud returns are dispersed to the seabed. If a heavy drilling fluid is required for drilling the interval, a relatively cheap drilling fluid is chosen, like a bentonite fluid system. This is because the economics of the pump and dump practice does not allow for an expensive mud system. To avoid shipping enormous amounts of mud to the drilling location offshore, typically a 16 ppg mud is diluted with seawater to produce a drilling fluid with the desired lowered density. But this practice also involves challenges in

deepwater areas regarding limitations of the rig, logistics and most of all concerns related to the mud quality. (Smith, Winters, Tarr, Ziegler, Riza, & Faisal, 2010)

The Riserless Mud Recovery (RMR) system developed by AGR, is the only DGD technology on the market as of today. The technology is used to return drilling fluid and cuttings from the well to the rig using a Subsea Pump Module (SPM) situated close to the seafloor and a Mud Return Line (MRL). This provides a closed loop mud circulation system without utilizing a marine riser. This allows for re-use and treatment of the drilling fluid which again makes it economically viable to use a more expensive and better suited drilling fluid system.

By using a better drilling fluid, a more stable tophole can be achieved. A better tophole with well-defined walls makes it easier to lower the casing string to the bottom. A gauge hole will also increase the chance of producing a good quality cement job, which results in a more stabile wellhead. The RMR technology is improving tophole sections in water depths up to 549m, but a successful field trail in the South China Sea in 2008 proved that a modified RMR system would work at a water depth of 1419m. (Smith, Winters, Tarr, Ziegler, Riza, & Faisal, 2010) (Rezk, 2013)

2.2 Post-BOP

In this subchapter the three different Post-BOP DGD systems will be presented.

2.2.1 Subsea Mudlift Drilling

To overcome the difficulties of drilling in deepwater environments from 1200- 3050m the SMD drilling system was developed. The Subsea Mudlift Joint Industry Project (1996-2001) was the first to deliver and prove the Subsea Mudlift Drilling technology. Being a closed system with no discharge to the environments, this technology is also a hot candidate for drilling in environmentally sensitive areas. (Østvik, 2011)

During SMD, the marine riser is filled with seawater or a fluid with seawater density. This reduces the amount of mud needed for the drilling operation, which saves mud maintenance costs and rig loads. A rotating diverter separates the seawater in the riser and the fluids contained in the wellbore. Cuttings and mud return are pumped to surface, through the return

line, with a set of subsea pumps located at the seafloor. These pumps take suction just below the rotating diverter, at the annulus side of the wellbore. The subsea pumps can operate in one of three modes; constant inlet pressure, constant circulation rate or manual override mode. During wellkill operations, the flexibility of operating the subsea pumps and their inlet pressure replaces the drilling choke. The return line is then used in the same way as the choke line in conventional drilling. (Schubert, Juvkam-Wold, & Choe, 2006)

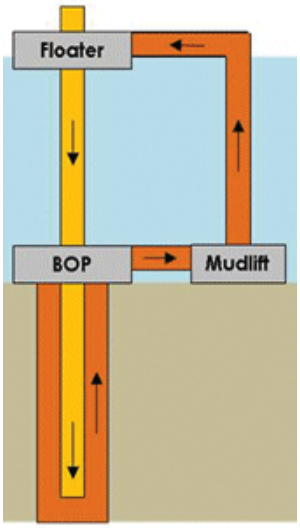

Figure 2-2. Subsea Mudlift Drilling

2.2.2 Dilution

Instead of pumping heavy mud from the sea floor to the surface with big pumps, the dilution-based dual gradient system can provide significant cost reduction as well as enhanced well control in deepwater wells by diluting the mud in the riser to create a different pressure profile at the sea floor. (MCS Kenny, 2013) (Mazerov, News: Drilling Contractor, 2012)

Transocean's dilution system, developed in collaboration with Dual Gradient Systems, the Continuous Annular Pressure Management (CAPM) system is designed to follow the earth's profile where the ocean exerts a relatively low pressure while the earth exerts a high pressure. The system is based on pumping a light drilling fluid either through the annulus created between the marine riser and an inner riser or through dedicated booster lines. By injecting the same mud as the drilling mud, but without barite, into the return mud stream at the bottom of the riser, a lower density mud column is achieved in the drilling riser. This creates two stable mud densities in the wellbore.

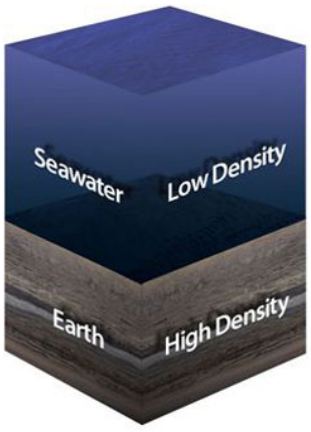

Figure 2-3. Earth's pressure profile (Mazerov, 2012)

By running a rotating control device (RCD) near the top of the riser below the slip joint, a closed loop system is created. The RCD holds back pressure and directs flow to the choke manifold while flow meters, monitoring flow in and out of the well, enable early detection of kicks and losses. A specially designed centrifuge separates the light dilution fluid from the heavier drilling fluid. The effect of the dilution system might not be as

big as the effect of the other DGD systems, but with the CAPM system all the necessary equipment is on the surface and can therefore be maintained and repaired quickly and efficiently resulting in very little downtime. If needed, the system can also be switched back to a conventional single gradient system within an hour. (Mazerov, News: Drilling Contractor, 2012) (MCS Kenny, 2013)

During comparative testing in the Gulf of Mexico a conventional single- gradient well included nine casing and liner seats to reach target depth (TD) in a deepwater well, while drilling with the CAPM system included only six casing and liner seats to reach the same TD. As stated by Luc de Boer, president of Dual Gradient Systems: "*The reduction in casing strings, at $10 million per string, is significant.*" (Mazerov, News: Drilling Contractor, 2012), (Ghiselin, 2012)

2.2.3 Controlled Mud Level

The controlled mud level (CML) system is the last of the three post-BOP dual gradient drilling classifications made by IADC. After the BOP and riser are in place the controlled mud level system is installed. The system includes a modified riser joint and a pump system to return cuttings and fluid from the wellbore back to the surface. The pump system is either attached to the riser or launched with a launch and retrieval system and suspended from the rig. As well as the other DGD systems described above, the controlled mud level (CML) system also utilizes fluids with different densities to control the downhole pressure. A significant difference is that the lower density fluid, in the upper part of the riser, may include gas.

The level of control over the wellbore pressure is dependent on where in the riser the CML system is placed as well as fluid density. The CML system is an open system as opposed to the other two post-BOP systems which have a rotating seal to create a closed system. By adjusting the level of heavy mud in the riser changes can be made to both the dynamic bottomhole pressure (BHP), for equivalent circulating density (ECD) effects, and the static BHP, for trip and connection margins. Increasing or decreasing the return pump rate with respect to the surface pump rate achieves the adjustment of fluid level in the riser. With this

system it is also possible to adjust ECD during cementing, completion and intervention operations. The CML system is used in intermediate water depth operations. (Statoil, 2014)

3 Advantages and challenges of dual gradient drilling technology

The dual gradient drilling technology includes several advantages over conventional drilling methods. In this chapter some of these advantages will be presented. Being a young technology, DGD also has some challenges associated with it. These challenges will also be presented here.

3.1 Advantages

The advantages of DGD include:

- By utilizing a heavier mud weight the slope of the downhole pressure gradient can be adjusted and might fit the geological pressure gradient better, compared to conventional drilling with a single fluid gradient. A pressure gradient more suited for the formation pressure will reduce the number of casing strings needed to reach the target depth.
- The use of fewer casing strings leaves a better footprint as well as saving time and reducing well cost. Dual gradient drilling has the potential of reducing well cost with as much as 50%.
- The reduction of casing strings needed allows for larger diameter wellbores to be drilled, which will accommodate larger production strings and potential designer completions. This will in turn increase production rate and improve well productivity.
- By monitoring the fluid level in the riser and the subsea pump rate, the DGD system achieves better kick/loss detection and reduces the likelihood of associated well control problems.
- DGD allows for optimal circulation rate for hole cleaning and rate of penetration (ROP). This is hard to achieve with conventional drilling, because the optimal circulation rate will often give a high ECD and might fracture the formation, but DGD can compensate for the increased ECD by lowering the fluid level in the riser and keep a constant BHP when the circulation rate is increased. Also, with DGD the heavier mud itself will in many cases improve well cleaning.
- The seawater in the riser will lighten the riser, reducing tensioning requirements.

- The heavier drilling mud used in DGD makes it possible to drill with a complete riser margin, which will reduce well control hazards associated with an emergency riser disconnect from the wellhead.
- Smaller rigs may be used to drill at greater water depths than before.
- Cost of drilling tophole sections is reduced with the RMR system. The RMR system also reduces the risk of shallow gas influx by enabling the use of weighted engineer mud as well as minimizing the environmental impact by eliminating the "pump and dump" practice.

(Herrmann & Shaughnessy, 2001) (Smith K., Gault, Witt, & Weddle, 2001) (Enhanced Drilling) (Smith, Winters, Tarr, Ziegler, Riza, & Faisal, 2010) (Drilling Contractor, 2011) (Gaup, 2012)

3.2 Challenges

These are some of the challenges associated with DGD:

- U-tubing effect:
  A high density mud in the drillstring and a lower density mud in the annulus results in an imbalance of pressure inside the drillstring and in the annulus. This pressure imbalance will cause the the mud to freefall inside the drillstring and u-tube into the annulus unless the rigpump circulation rate is greater than the mud freefall rate. This u-tube effect can disguise well influxes or lost circulation, which will increase the risk associated with drilling the well. Understanding and managing the u-tube effect is therefore a primary goal of all drilling and well control procedures. (Smith K., Gault, Witt, & Weddle, 2001) (Schubert, Juvkam-Wold, & Choe, 2006)

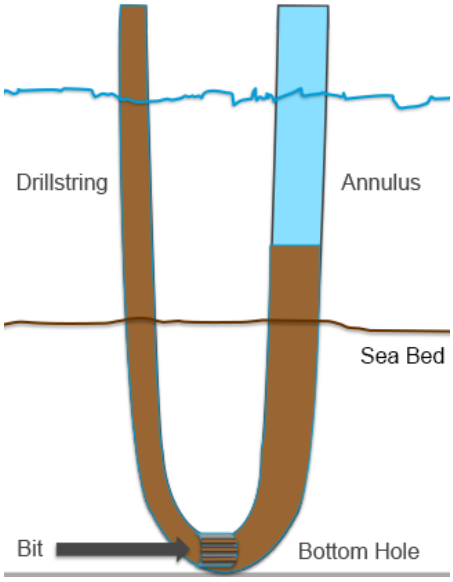

Figure 3-1. U-tube effect

- As most of the DGD equipment is subsea equipment, repairs and maintenance must be done under water or by lifting the equipment to the surface first, which is more challenging and time consuming compared to topside equipment.

- The pressure difference between the low density fluid, or gas, used in the riser and the hydrostatic pressure exerted by the seawater on the outside of the riser, makes it necessary to assess the risk of riser collapse.
- The petroleum industry often has a conservative mindset, which in itself can present challenges:
    - The industry is generally less receptive to changes such as DGD.
    - The risk associated with applying such a new technology as DGD, might be perceived as too high for the potential gain.
    - Personnel training is needed before the DGD system can be put into use.
- Some DGD systems require more power than conventional drilling. Most rigs would need an extra diesel generator to increase the power capacity, which would take up more rig deck space.
- Modifications to the rig are needed to accommodate the new equipment used with DGD.

(Drilling Contractor, 2011) (Rezk, 2013) (Gaup, 2012)

4 Dual gradient drilling equipment

Much of the equipment used in DGD is similar or the same for several of the DGD methods. This chapter will present the primary elements needed for DGD operations.

4.1 Subsea pump module

Providing a support frame for the pumps, motors, hose interfaces and control systems, the subsea pump module (SPM) is one of the most essential parts of all DGD systems, except for the dilution system. Although there are differences between the SPM used for the different DGD systems, the principle is the same. The SPM receives the mud return flow from the well and pumps mud and cuttings back to the surface for processing.

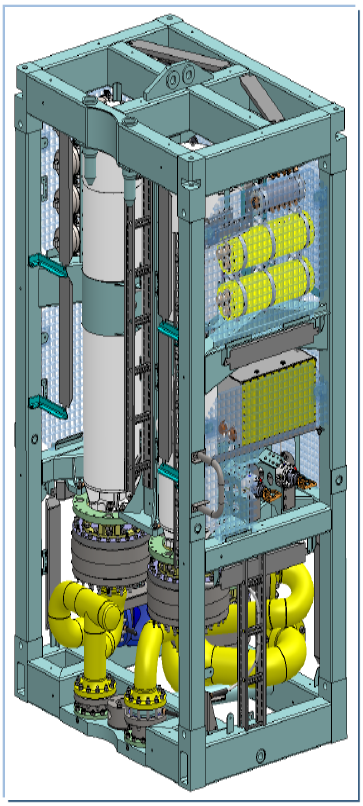

Figure 4-1. Subsea pump module (Statoil, 2014)

The pump in the SPM can be set to a constant inlet pressure mode where the pump automatically and accurately regulates the pressure according to the pressure conditions in the well. The pump can also be run in a constant flow rate mode or a manual override mode. The pump is either driven by an electric motor or by seawater pumped from a seawater pump on the rig through a seawater supply line to the SPM. All SPM settings can be controlled from the surface through an umbilical.

The depth at which the SPM is installed depends on the DGD method. The seabed pumping method and the RMR method has the SPM installed close to or on the seabed. During controlled mud level operations the SPM is installed on a modified riser joint closer to the surface in order to adjust the level of mud in the riser. (Brown, Urvant, Thorogood, & Rolland, 2007) (Østvik, 2011) (Smith, Winters, Tarr, Ziegler, Riza, & Faisal, 2010) (Smith K., et al., 1999) (Dowell J., 2010) (Dowell D., 2011)

4.2 Mud return line

The MRL is the conduit that transfers return fluid and cuttings from the seabed to surface. The MRL is most commonly a 6" diameter soft rubber hose that is designed to withstand forces exerted by currents and rig movement. The MRL is either installed separately or integrated into the riser. If the MRL is run as an integrated part of the riser, each riser joint will be modified to include an additional fixed line in a free slot.

The 6" mud return line is smaller than the area of the riser annulus and the mud is transported to the surface faster than it would with conventional drilling. The faster flow speed reduces the exposure time of the mud in cold temperature thereby reducing the risk of mud properties degrading. (Østvik, 2011) (Rajabi, Toftevåg, Stave, & Ziegler, 2012) (Fossli & Stave, 2014)

4.3 Drill string valve

Located near the bit in the bottomhole assembly (BHA) the purpose of the drill string valve (DSV) is to prevent the mud in the drillpipe from u-tubing into the well when circulation is stopped during connections. The valve is spring-loaded and opens at a preset force exerted by the positive pressure from the rig pumps. When circulation stops, the force on the spring drops and the valve closes to prevent the u-tube effect. Although the DSV is not an essential part of the SMD tool package, it makes the operations easier by allowing for faster connections and better certainty in kick detection. The DSV comes in several sizes suitable for different drill pipe sizes and can be used in water depths ranging from 3050m to 10 700m. (Dowell D., 2011) (Schubert, Juvkam-Wold, & Choe, 2006) (Dowell J., 2010)

4.4 Solids Processing Unit

The solids processing unit (SPU) is one of the essential parts of the seabed pumping system. The SPU is part of a special riser joint and provides feed of mud to the SPM. The pump can not handle big solid pieces, so the SPU is designed to crush solids into sizes of 1" to ½" or smaller, a size that the pump can handle. Solids already smaller than this will pass through the SPU without being affected. From the SPU, mud and cuttings are fed to the SPM to be pumped back to the surface. Several valves are available for controlling the flow into the SPM and, if needed, for flushing the SPU. (Dowell D., 2011) (Dowell J., 2010)

4.5 Suction Module

During drilling with the RMR system, the riser has not yet been run. The cylindrical open topped suction module (SMO) is used during RMR drilling and provides access to the well for the drill pipe and works as a receiver for return mud and cuttings exiting the wellhead. The hydrostatic pressure from the seawater above and the speed of mud delivery by the underwater pump stabilizes the drilling mud in the SMO. The SMO is connected to the SPM with a flexible suction hose that is made up by the remotely operated vehicle (ROV). The SMO is deployed on the drillstring, through the rig's moonpool, and mounted on the wellhead. Different models of the SMO are provided for different wellhead designs.

Figure 4-2. Suction Module

To monitor the level of mud in the SMO it is fitted with lights and cameras as well as a pressure transducer to register the hydrostatic pressure of the mud column in the SMO. The pictures from the cameras and the hydrostatic pressure readings from inside the SMO makes it possible for computers to control the mud level in the SMO to a constant level. This constant level means that mud and cuttings are pumped up to surface at the same rate they exit the wellbore and no cuttings or mud is left on the seafloor. The cameras are also used to monitor the amount of shallow gas and drilled gas escaping from the well. This gas can be seen as bubbles rising from the mud in the SMO. (Smith, Winters, Tarr, Ziegler, Riza, & Faisal, 2010)

4.6 Subsea Rotating Device

The subsea rotating device (SRD) is located above the solids processing unit and, as the uppermost piece of equipment in the seabed pumping system, it provides an interface between the riser and the wellbore. The function of the SRD is to separate the seawater in riser from the higher density fluid in the wellbore. The SRD also ensures that gas does not enter the riser and that the well is slightly pressurized, usually with about 3,5 bar, in order to feed the SPM. The sealing element of the SRD can hold pressure from below up to 138bar during static and 69 bar

Figure 4-1. Subsea rotating device

(1000psi) when rotating. The SRD can also hold pressure from above up to 69 bar both during static and when rotating. The seals and bearings in the SRD are retrievable and during each drillpipe trip these parts will be run on the drillstring to the surface for maintenance and servicing. (Dowell D., 2011) (Dowell J., 2010)

4.7 Riser Dump Joint

During an emergency riser disconnect, the SRD would trap the riser fluid in the riser and not allow free flow in and out of the riser as would happen with conventional systems. Analyses have shown that an emergency riser disconnect with trapped riser fluid inside would significantly increase the loads on the riser. During rough sea states these loads might become too great for the riser system to withstand. The solution to this problem is to install a riser dump joint (RDJ), which will open and allow free fluid flow in and out of the riser tube to reduce riser loading in case of an emergency riser disconnect. (Dowell J., 2010)

4.8 Top Fill Pump

The top fill pump is used during controlled mud level drilling to provide downward mud stream into the riser above the subsea pump outlet in order to increase the mud level in the riser, if needed. It is possible to increase the mud level without the top fill pump, by running the SPM at a lower rate than the mud pump, but by utilizing the top fill pump a quicker level adjustment can be achieved. The top fill pump is also used to increase the riser mud level during connections when mud circulation is stopped.

The top fill pump will constantly circulate the mud above the mud outlet in the riser, which conditions the mud and avoids mud sag. In addition, the continuous downward mud flow also provides cooling of the slip joint and creates a mud wall which stops potential accumulated gas in the riser from reaching the drill floor. Gas sensors are installed in the vent lines and the flow line on the rig to continuously measure the amount of free gas in the evacuated part of the riser. These sensors can be set to trigger a warning or an alarm if the amount of gas in the riser approaches dangerous levels.

During drilling there is a possibility that sparks can be created from the interaction between the drill pipe and the diverter box, mud funnel or riser, which in turn could ignite the gas and

create a fire. The downward mud stream from the top fill pump provides a moist environment in the riser, which prevents sparks and a potential fire. (Rajabi, Rohde, Maguire, Stave, & Tapper, 2012) (Fossli & Stave, 2014) (Statoil, 2014) (Sigurjonsson, 2012) (Statoil, 2013)

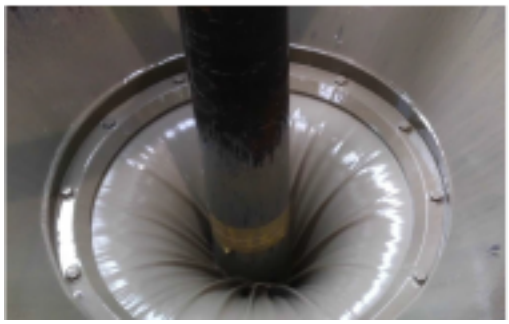

Figure 4-4. Mud seal (Fossli & Stave, 2014)

5 Challenges during connection operations

To do connections during drilling operations requires that you either have a continuous circulation unit or that you have to compensate for the annulus friction pressure loss. This chapter will present some challenges associated with connection operations. The subject of a continuous circulation system will not be covered in this thesis.

5.1 Overview

During conventional drilling, before a connection is made, the mud circulation has to be stopped. This causes a rapid drop in the mud pressure before it stabilizes at the static level. This quick pressure drop may put the well in underbalance, which can lead to inflow from the formation in the exposed wellbore. After the connection has been made circulation can continue. When circulation continues it causes a rapid pressure increase, before it decreases to stabilize at the circulating level. The pressure increase can exceed the fracture pressure of the formation and damage the formation in the uncased part of the wellbore.

In conventional drilling this stop-start circulation is repeated every 30- 60 or 90 ft when a new connection is made. This leads to the exposed formation repeatedly being first depressurized when circulation is stopped then pumped back up before normal circulation pressure again is established. The various MPD technologies tries to compensate for the pressure variations experienced in the wellbore during connections.

The next subchapter will present some problems that may be encountered when circulation is stopped during a connection procedure.

5.2 Formation fracturing

When the hydraulic pressure in the wellbore exceeds the fracture pressure of the formation, the formation can fracture and fluid will penetrate the surrounding formation. After fracturing has occurred fluids will be absorbed by the formation at a lower pressure than the initial fracture pressure.

To avoid formation fracturing the circulating pressure must be kept between the pore pressure gradient and the fracture pressure gradient during connections. This can be especially

challenging when stop- start circulation produces a varying ECD across the exposed formation surface. (Maris, 2009)

5.3 Formation pumping and ballooning

Another negative effect of the downhole pressure being changed up and down repeatedly is formation pumping. The most extreme causes of formation pumping can charge up the formation with injected fluid or even fracture it. The formations ability to return this fluid to the wellbore, when circulation is stopped, is called ballooning and can be misinterpreted by the driller as a kick. (Maris, 2009)

5.4 Lost circulation

Lost circulation is a term used for circulation fluid that is lost into the formation, and is experienced as a reduction in mud flow return. In a fractured or porous formation, the size of the lost circulation depends on the positive differential pressure of the circulation fluid over the formation pressure.

Loss of mud to the formation will naturally increase the well cost, but in addition, lost circulation will reduce the circulation pressure, which may lead to a kick somewhere else in the wellbore. (Maris, 2009)

5.5 Connection kick and formation collapse

During conventional connection operations the downhole pressure can drop 30-40 bar under normal circulation pressure, which can cause influx of formation fluid into the wellbore called a connection kick. It is also possible that the pressure drop can initiate a formation collapse. The risk of connection kicks or formation collapse when drilling with a DGD system is drastically reduced as the downhole pressure drop is usually lower than five bar when making connections.

With a DGD system, as well as with conventional drilling, there is still a risk that a connection kick will not be immediately detected, since there is no way of monitoring the BHP when circulation is stopped. Measurements of BHP is sent back to the surface with mud pulses, which is not possible without circulation. (Maris, 2009)

5.6 Differential sticking

Differential sticking is a condition where the drill string gets stuck against the hole wall and cannot be rotated. This usually happens in a highly permeable formation where there is a high pressure differential across a nearly impermeable filter cake between the wellbore and the formation. The problem can be very costly because of the non-productive time (NPT) on the rig.

While trying to free the stuck pipe, the drill string might part, which will call for a fishing job or side tracking and even more NPT. Also, connections made during these attempts can reduce the mud pressure, which in turn can lead to a kick. (Maris, 2009)

5.7 Stuck pipe

When the bit, collars, bottom hole assembly (BHA) or the drill pipe for some reason gets stuck in the wellbore, it is called a stuck pipe. This situation may be caused by a collapsing borehole wall, or formation being deformed inwards and reducing the hole size, which are both triggered by stop- start mud circulation during connections. In addition, unless a high gel strength mud is used, cutting and debris can settle in a vertical hole when circulation I stopped and cause stuck pipe. However, using a mud with high gel strength can subject the wellbore to a higher initial pressure surge when circulation starts up after the connection operation. (Maris, 2009)

5.8 Slugging of cuttings return

When circulation is stopped during connections, cuttings and debris will settle and mud can heat up downhole and may change its properties. This is especially challenging in high-pressure and high-temperature wells, as the change in mud properties can significantly affect hydraulic calculations, pressure, circulation rate etc.

When circulation continues there will be considerable variations in the mud as well as the cuttings across the shale shakers. This problem can be reduced by continuing circulation after drilling has stopped, until cuttings have been circulated above the drill collars in the annulus. (Maris, 2009)

5.9 Narrow fracture/ pore pressure windows

All MPD methods aim to keep the BHP constant when circulation is stopped. This can be challenging because of the dynamic pressure drop in the open hole between the bit and the last casing shoe. When the circulating pressure gradient is close to the fracture pressure at the last casing shoe and close to the pore pressure at the bit, the section needs to be cased. When drilling conventionally in deep waters, especially, this will result in a large number of casings needed to reach target depth. The DGD method creates a pressure gradient more similar to that of the formation in order to reduce the number of casing strings needed. (Maris, 2009)

6 Control Theory

This chapter is focused on presenting the control theory used for DGD in order to automate the connection procedures during drilling operations.

6.1 Linear control

Linear control algorithms are used in typically 95% of all industrial control applications. A feedback controller is used to bring the operating condition of a process to a predetermined reference value. This is done by changing the controller output value based on the difference between the measured value and the reference value, which is called the error. The purpose of the control algorithm is to reduce the error signal in the system to zero and maintain the set reference value. The error signal is given by

$$e = r - y$$

Where:

e is error signal

r is reference value

y is measured value

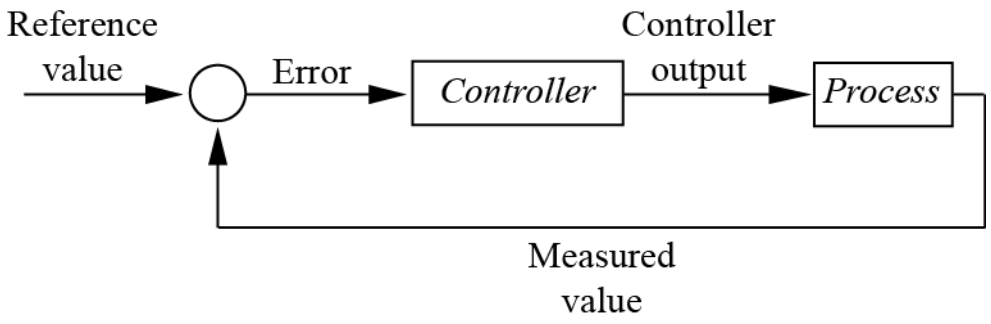

Figure 6-1. Linear Control

Several controllers are available today, but these are the most used:

- *Proportional* (P): This is the simplest controller, where the controller output is proportional to the input error signal. This means that changes in output are proportional to the current error value. The process will reach its reference value

quicker with a higher proportional gain, but if the proportional gain is to great, the system may become unstable. The proportional term is given by

$$u = u_0 + K_p e$$

Where:

u is the controller output

u_0 is the input value

K_p is the proportional gain

- *Integral* (I): Also known as *reset control*, the integral controller performs integration on the input error signal to change the measured value at a rate proportional to the error. The integral term accumulates all the previous errors and their durations to speed up the changes in output to reach the reference value quicker. If the error is positive the accumulated errors will increase and if the error is negative the accumulated error will decrease. At any time, the accumulated error count will be the reset contribution to the measured value. If the contribution of the integral term is too high it may result in an overshoot of the process output compared to the reference value. The integral term is given by

$$u = K_p \frac{1}{T_i} \int_0^t e \, d\tau$$

Where:

T_i is the integral time constant

- *Derivative* (D): The derivative term is also known as *rate control* and works as a means of suppressing the overshoot that the integral term sometimes causes, by considering the change of the input error signal and slowing down this change rate of the controller output. The derivative term is given by

$$u = K_p T_d \dot{e}$$

Where:

T_d is the derivative time constant

When we combine these three components we get what is called a PID controller, given by

$$u = u_0 + K_p e + \frac{K_p}{T_i}\int_0^t e\,d\tau + K_p T_d \dot{e}$$

The figure below illustrates how the PID controller works to reduce the error signal in the system and maintain the set reference value. The three components are rarely used separately but for most applications it is sufficient to use the first two terms, without the derivative term. The controller is then called a PI controller where the T_d value is set equal to zero. (Güyagüler, Papadopoulos, & Philpot, 2009) (Saeed, Lovorn, & Knudsen, 2012) (Nygaard & Godhavn, Automated Drilling Operations , 2013)

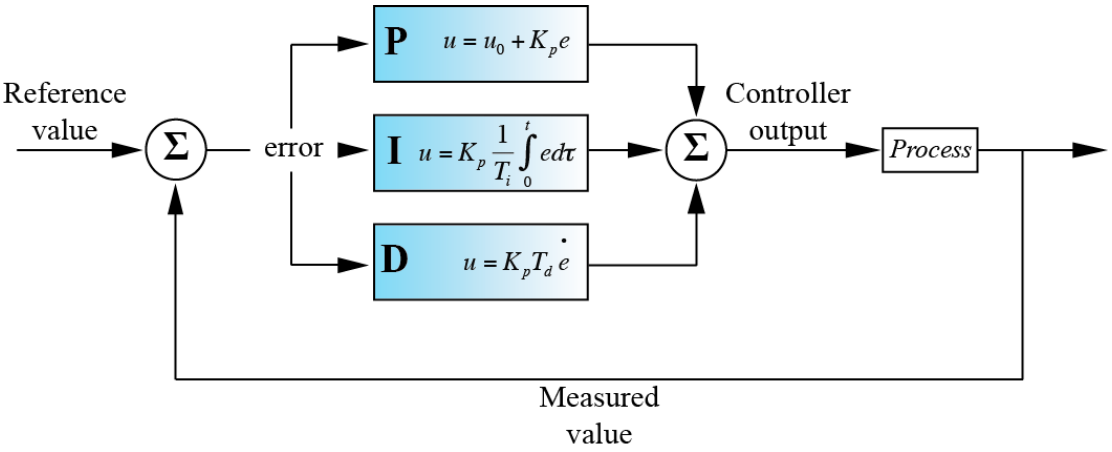

Figure 6-2. PID controller

6.2 Feedforward control

When using a regular PID feedback controller the reference value is always a constant value and the controller has no knowledge of the actual process. Control loops are often affected by disturbances and a feedback controller can only take action based on the result of the disturbance. This means that when a disturbance affects the system, the feedback controller cannot do corrections until after the system output has been affected.

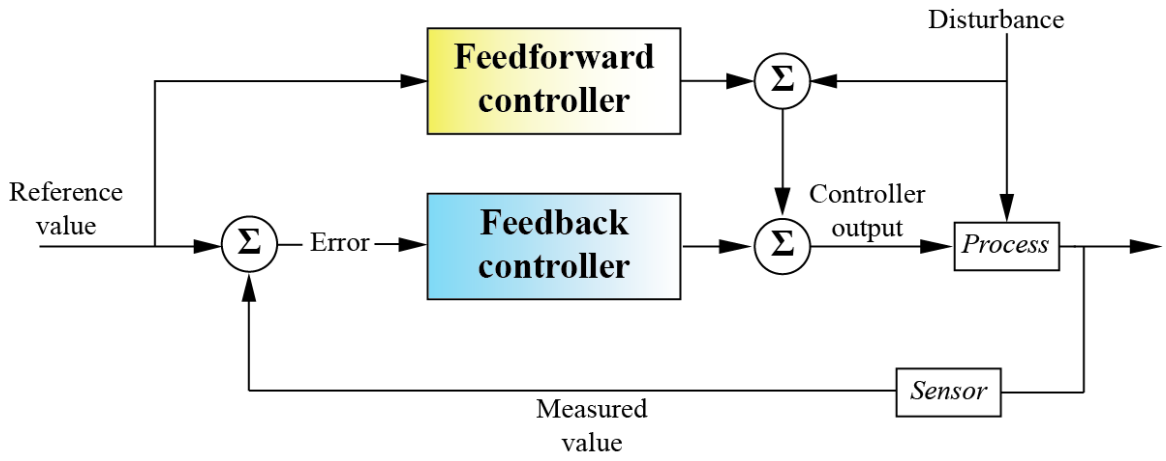

Figure 6-3. Feedforward control

If the process experiences a disturbance, v, or a change in reference value, r, a feedforward controller can be applied to improve the control properties and performance. By measuring the disturbance, the feedforward controller will act the moment a disturbance occurs and quickly make corrections to reduce the effect of that disturbance before it shows up in the system output signal. A feedforward controller can be used in various ways, but is usually distinguished between feedforward from the reference and feedforward from the disturbance. The PID- controller with feedforward is given by

$$u = u_0 + K_p e + \frac{K_p}{T_i}\int_0^t e\,d\tau + K_p T_d \dot{e} + K_r \dot{r} + K_v v$$

Where:

$K_v v$ is feedforward term for changes in the disturbance

$K_r \dot{r}$ is feedforward term for changes in the reference

The ideal feedforward controller would include a model of the process in order to make exact corrections according to the disturbance, thus eliminating the need for a feedback controller. Since the feedforward controller is not able to give such exact compensations, the feedforward controller is almost always included as an addition to the feedback controller. With this setup the objective of the feedforward controller is to reduce the effect of the major disturbances while the feedback controller takes care of other things that might cause the

system output to deviate from the reference signal. (Smuts, 2011) (Nygaard & Godhavn, Automated Drilling Operations , 2013) (Nygaard, 2014)

6.3 Ziegler-Nichols controller tuning

To make the PID controller perform as good as possible, its parameters K_p, T_i and T_d needs to be tuned to the correct value. This parameter tuning is actually the most critical step of constructing a control system. The tuning of the PID controller is done with a series of tuning experiments and the empirical values resulting from these experiments.

The Ziegler-Nichols tuning method is carried out as follows:

1. T_i value is set to a very high value and T_d is set equal to zero in order to disable the integral and derivative terms.
2. With a varying K_p, runs are performed until oscillations with constant amplitude and frequency occur.
3. The K_u value (ultimate gain) is recorded.
4. The period length between oscillations, referred to as T_u value is recorded.
5. The controller parameters are calculated using the empirical formulas given in table 1.

Table 1. Ziegler- Nichols controller tuning

Controller	K_p	T_i	T_d
P	$K_u/2$	∞	0
PI	$K_u/2.2$	$T_u/1.2$	0
PID	$K_u/1.7$	$T_u/2$	$T_u/8 = T_i/4$

Because the process response usually changes over time, it is often hard to achieve oscillations with constant amplitude and frequency. Therefore, an averaged period length of the oscillations seen is generally sufficient to be used for calculations. (Güyagüler, Papadopoulos, & Philpot, 2009) (Nygaard & Godhavn, Automated Drilling Operations , 2013)

6.4 Drilling fluid tank example

To illustrate the control theory a tank system can be simulated using a dynamic model of the tank level and valve operation, where the drilling fluid level in the tank is dependent on the flow rate in, q_{in}, and the valve opening, Z_c. The tank in question has a height of h meters and an area of A square meters.

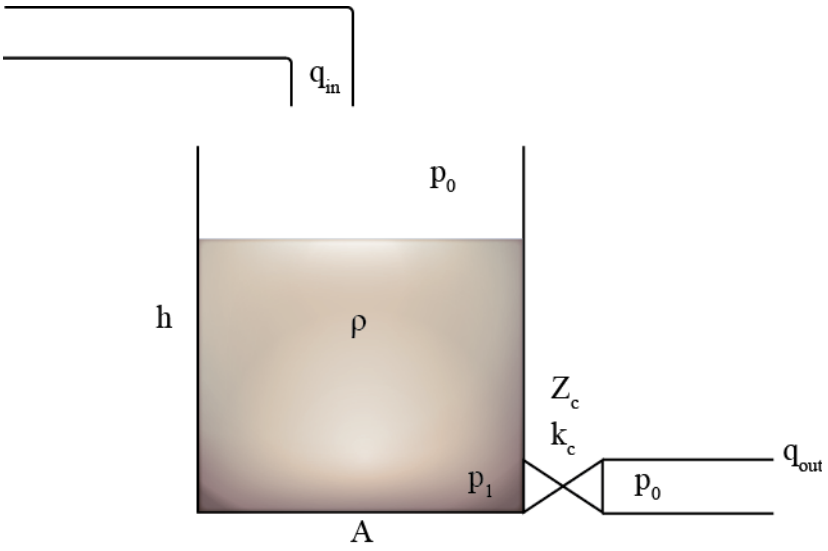

Figure 6-4 Tank level control

The dynamic model is described in Figure 6-4.The parameters for the simulation are given in Table 2.

Table 2. Tank simulation parameters

Parameter	Value
Drilling fluid density	1620 kg/m^3
Tank area	10 m^2
Tank height	1,2m
Valve parameter, K_c	0,14
Valve opening, Z_c	1

6.5 Tank example without controller

This first example shows how the level in the tank changes with varying q_{in}, when no controller is added to the system. The simulations are based on the following equations:

Tank level dynamics:

$$\dot{h} = \frac{1}{A}\left(q_{in} - q_{out}\right)$$

Tank level:

$$h_{(t+1)} = h_t + \dot{h}T_s$$

Flow rate out when p_0 is atmospheric pressure:

$$q_{out} = z_c k_c \sqrt{gh}$$

Where:

k_c is the valve constant

z_c is valve opening

g is the Earth's gravity

h is the tank level

The Euler's method is used when simulating the level in the tank, given by

$$h\left(t_{k+1}\right) = h\left(t_k\right) + \left[\frac{1}{A}\left(q_{in} - z_c k_c \sqrt{gh}\right)\right]dt, x\left(t_0\right) = 0$$

(Nygaard & Godhavn, 2013)

MATLAB is the software used to do these simulations.

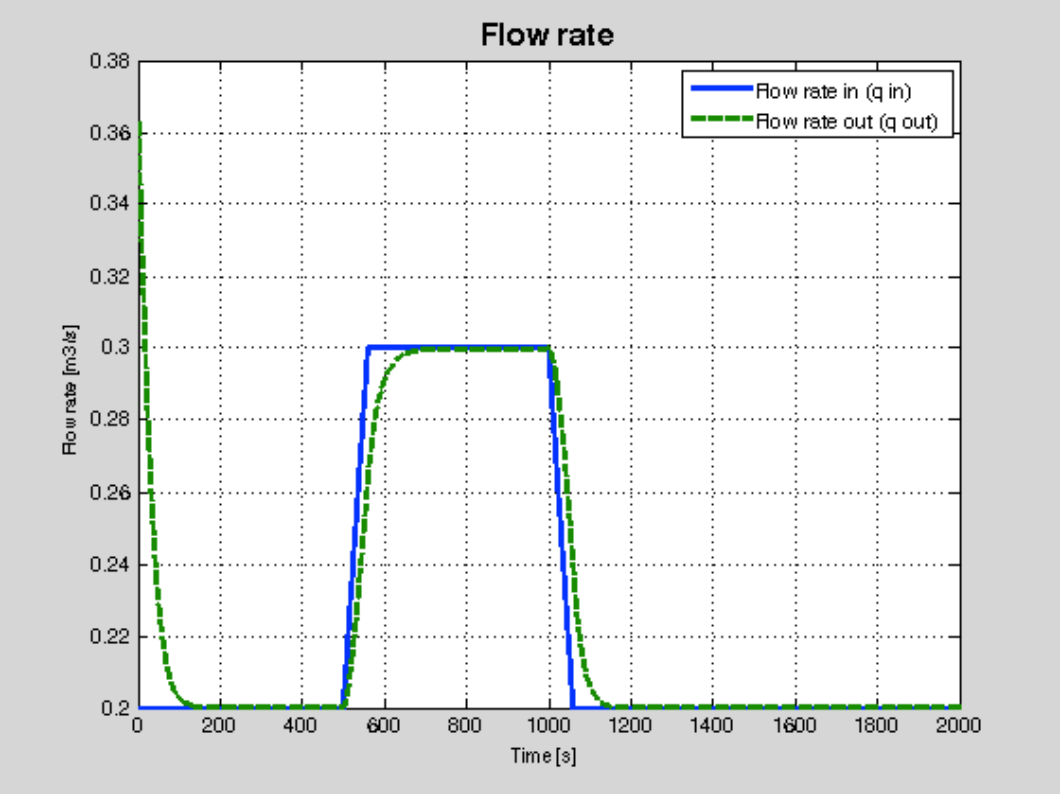

Figure 6-5 Flow rate in and out

With no controller there is no way to maintain a constant tank level with changing flow rates. The fixed valve opening will make the flow rate out follow the flow rate in, with a small delay, as seen in Figure 6-5. Figure 6-6 shows how the tank level also responds to the flow rate in with the same curve as the flow rate out.

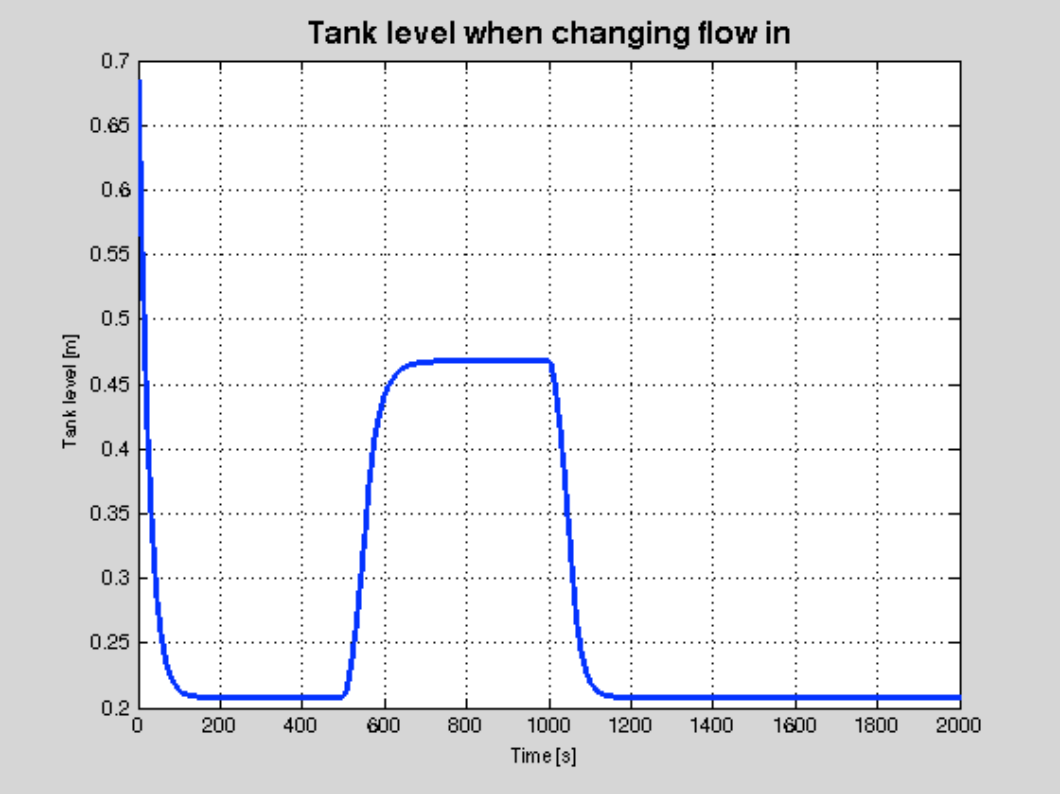

Figure 6-6 Simulations of drilling fluid tank level

6.6 Tank example with level controller

In order to describe the control theory in the previous subchapters, this subchapter is used to show how the drilling fluid level in a tank can be controlled automatically.

The same tank model as above will now be fitted with a PI controller, with feed forward from both the reference and from the disturbance, to illustrate the effect on the drilling fluid level in the tank with changing flow rates. In this example the reference value is set to h=0,4m, which is changed to h=0,1m after 500 seconds. To maintain the reference tank level the choke valve opening will be regulated by the PI controller to compensate for changes in flow rate and the reference change.

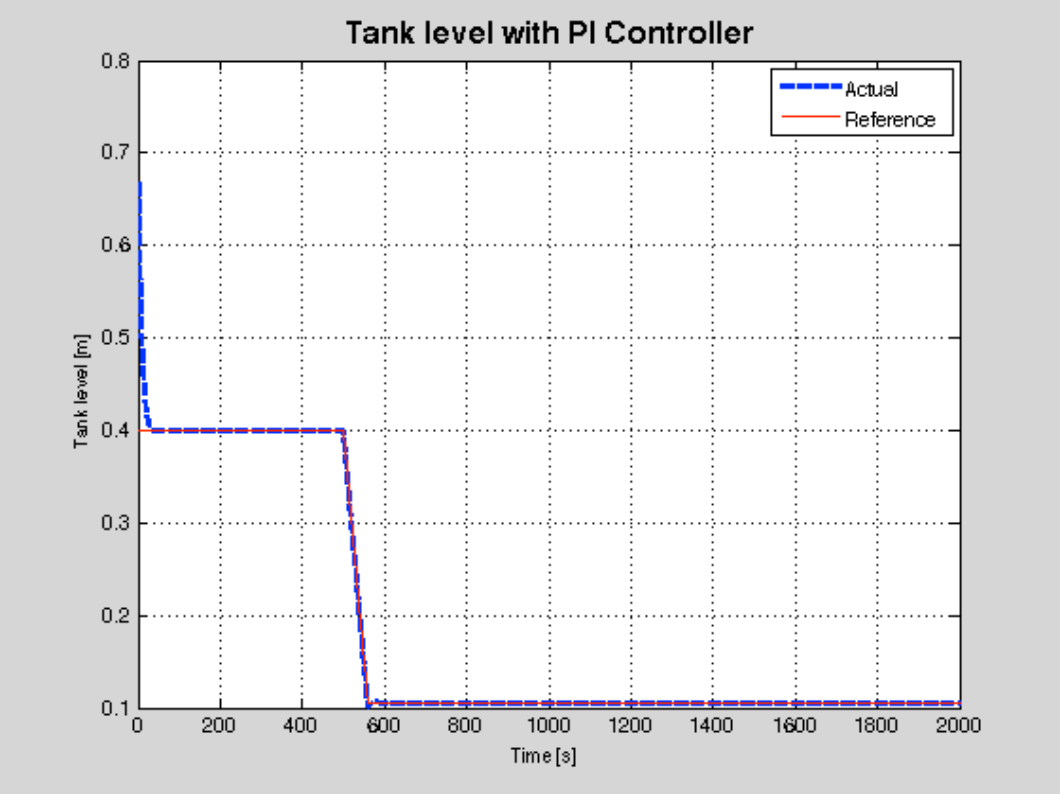

Figure 6-7. Tank level with PI controller

Figure 6-7 shows that with fairly well tuned K_p and T_i values the tank level reaches the reference level pretty quickly and stays on the reference line the whole duration of the simulation.

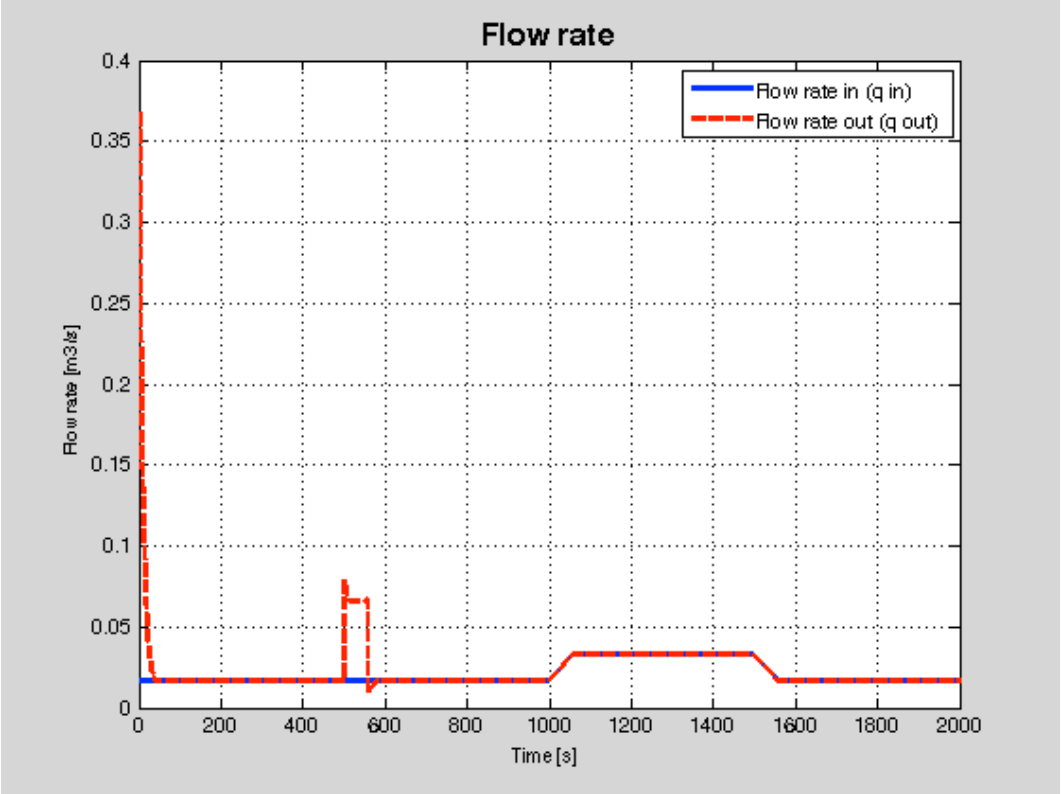

Figure 6-8. Flowrate

When the tank level reference is changed after 500 seconds we see an instant increase in the flow rate out of the tank. This is the result of the PI controller opening the choke valve to increase the flow rate out and reduce the tank level to the new reference level.

The flow into the tank is seen as disturbance by the system and the feedforward control immediately makes changes to the valve opening, when the flow rate in is altered, to minimize the error signal. This can be seen when comparing Figure 6-8 and Figure 6-9 at 1000 seconds.

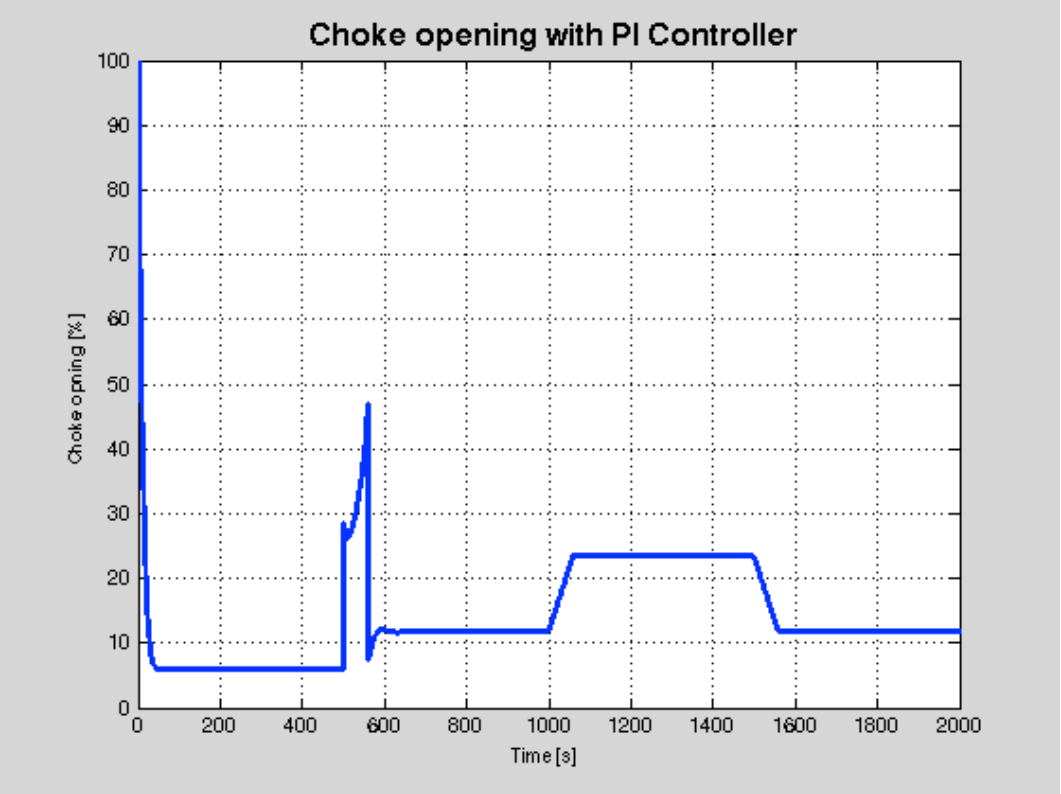

Figure 6-9. Choke opening with PI controller

By adding a PI controller to the tank example we see that the system can be easily controlled to maintain a constant tank level. Because the accuracy of the controller in this example is fairly good there is no need to add the derivative term to the controller, which would have complicated the system unnecessarily. In this example the disturbance, q_{in}, can both be measured and controlled, which greatly simplifies the task of maintaining a constant tank level. In a different system the disturbance might be uncontrollable and non adjustable. In that case the derivative term can be added to the controller in an attempt to reduce the error.

7 Wellbore Modeling

This chapter describes how the wellbore pressure dynamics and flow dynamics is modeled using the Kaasa model.

7.1 Kaasa model based simulations for MPD

In order to automate the control system used during an MPD operation, a hydraulic model is needed. Even though several advanced hydraulic models have been developed, the complexity of theses models can also be a downside. While capturing all aspects of the drilling fluid hydraulics, their complexity requires expert knowledge to operate. Because of the continuously changing conditions during an MPD operation the number of measurements taken may not be enough to keep all the parameters calibrated. In addition, the overall accuracy achieved with these complex models is not greatly improved.

Glenn-Ole Kaasa has developed a simplified hydraulic model, which uses basic fluid dynamics to describe the most important hydraulics of an MPD system. Because dynamics are really what complicate a model, unnecessary dynamics are neglected in the Kaasa model and only the dominating dynamics of the system are included. To simplify his model, Kaasa has removed dynamics which changes faster than the control system can react, removed slow dynamics which is easily handled by feedback from the measurement, and lumped together parameters that are impossible to differentiate.

The Kaasa model works by assuming that the flow pattern in the drill string is uniform throughout the whole length of the drill string and similarly that the flow pattern in the annulus is uniform throughout the whole length of the annulus. This way the well can be divided into two separate control volumes with different dynamics. (Kaasa, Stamnes, Imsland, & Aamo, 2011) (Nygaard & Godhavn, 2013)

The Kaasa model is typically presented with the following equations:

Pump pressure dynamics:

$$\dot{p}_p = \frac{\beta_d}{V_d}\left(q_p - q_b\right)$$

Choke pressure dynamics:

$$\dot{p}_c = \frac{\beta_a}{V_a}\left(q_b + q_{res} + q_{bpp} - q_c - \dot{V}_a\right)$$

Dynamics of flow rate through the bit:

$$\dot{q}_b = \frac{1}{M}\left(\left(p_p - p_c\right) - \left(F_d + F_b + F_a\right)q_b^2 + \left(\rho_d - \rho_a\right)gh\right)$$

Where:

q_p is flow rate from the pump

q_b is flow rate through the bit

q_{res} is flow rate from the reservoir

q_{bpp} is flow rate from the backpressure pump

q_c is flow rate through the choke, given by

$$q_c = z_c k_c \sqrt{\frac{p_c}{\rho_a}}$$

Where:

p_c is choke pressure

ρ_a is density of fluid in annulus

Wellbore parameters:

β_d is bulk modulus of the drill string

V_d is volume of the drill string

β_a is bulk modulus of the annulus

V_a is volume of the annulus

M is the integrated density per cross- section over the flow path

F_d is drill string friction coefficient

F_b is bit friction coefficient

F_a is annulus friction coefficient

ρ_d is density of fluid in the drill string

(Nygaard & Godhavn, 2013)

The BHP, in conventional drilling, is the seen as the sum of the hydrostatic pressure, H_p and the frictional pressures F_p. During circulation this gives

$$BHP_{dyn} = H_p + F_p$$

When circulation is stopped and frictional pressure drops to zero:

$$BHP_{stat} = H_p$$

In DGD and MPD the BHP is determined as follows

For **MPD**:

$$BHP_{dyn} = H_p + F_p + B_p$$

$$BHP_{stat} = H_p + B_p$$

Where

B_p is pressure applied from backpressure pump

For **DGD**:

$$BHP_{dyn} = H_{p,total} + F_p$$

$$BHP_{stat} = H_{p,total}$$

Where:

$$H_{p,total} = H_{p,fluid1} + H_{p,fluid2}$$

7.1.1 Example with constant choke

Subchapters 7.1.1 and 7.1.2 describes the Kaasa model used in an annulus back pressure setup. Two examples are presented. First with a constant choke, second with an active choke controller.

To simplify the simulations in this chapter the true vertical depth (TVD) of the well will be considered constant throughout the length of the simulation.

The wellbore parameters for the simulations are given in Table 3.

Table 3. Wellbore parameters

Parameter	Value
ρ_a	1580 kg/m3
ρ_d	1580 kg/m3
β_d	$2e^9$
β_a	$1e^9$
V_d	17 m^3
V_a	48 m^3
M	$4.3e^8$
F_d	$5e^9$
F_b	$1e^9$
F_a	$2e^9$

The parameters ρ_a and F_a are considered known is this thesis as there is no influx included in the simulations.

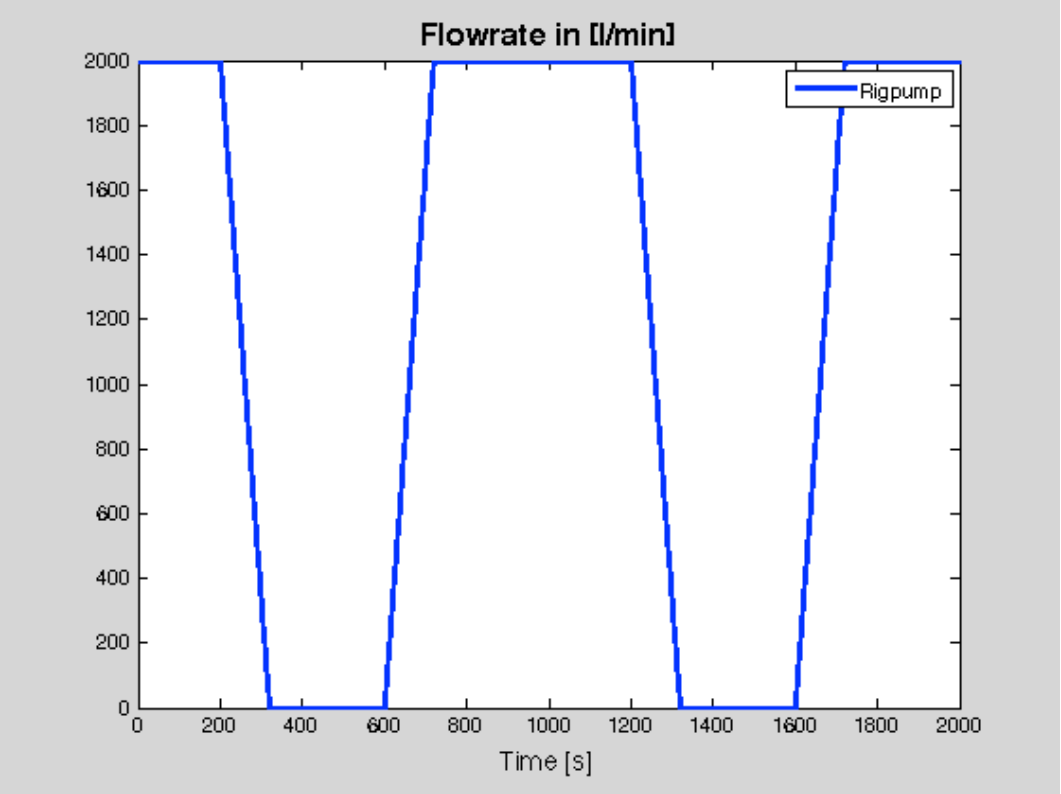

Figure 7-1. Flowrate in (l/min)

To simulate a connection operation the rig pump is ramped down from 2000 l/min to zero in two minutes, starting at 200 seconds. At 600 seconds the rigpump is ramped back up to 2000 l/min in two minutes. The same events are repeated at 1200 seconds.

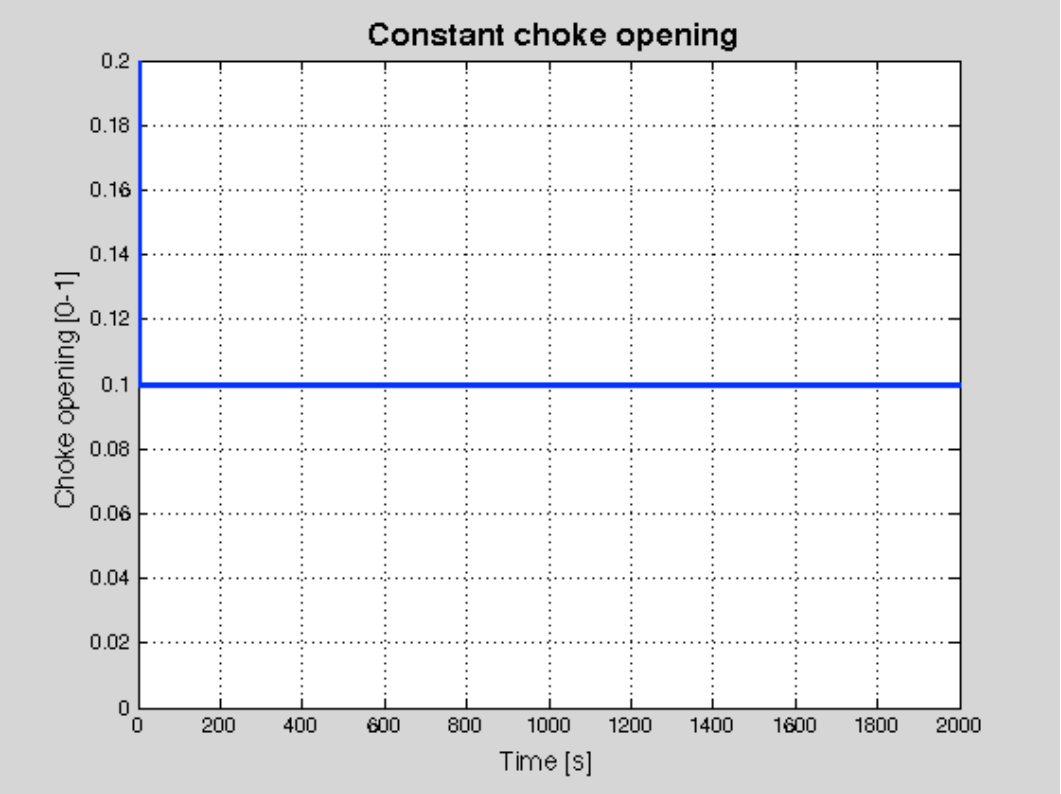

Figure 7-2. Constant choke opening

This simulation is run with a constant choke opening at 10% open, as shown in Figure 7-2, to illustrate a conventional drilling operation and how the downhole pressure is affected during connection operations.

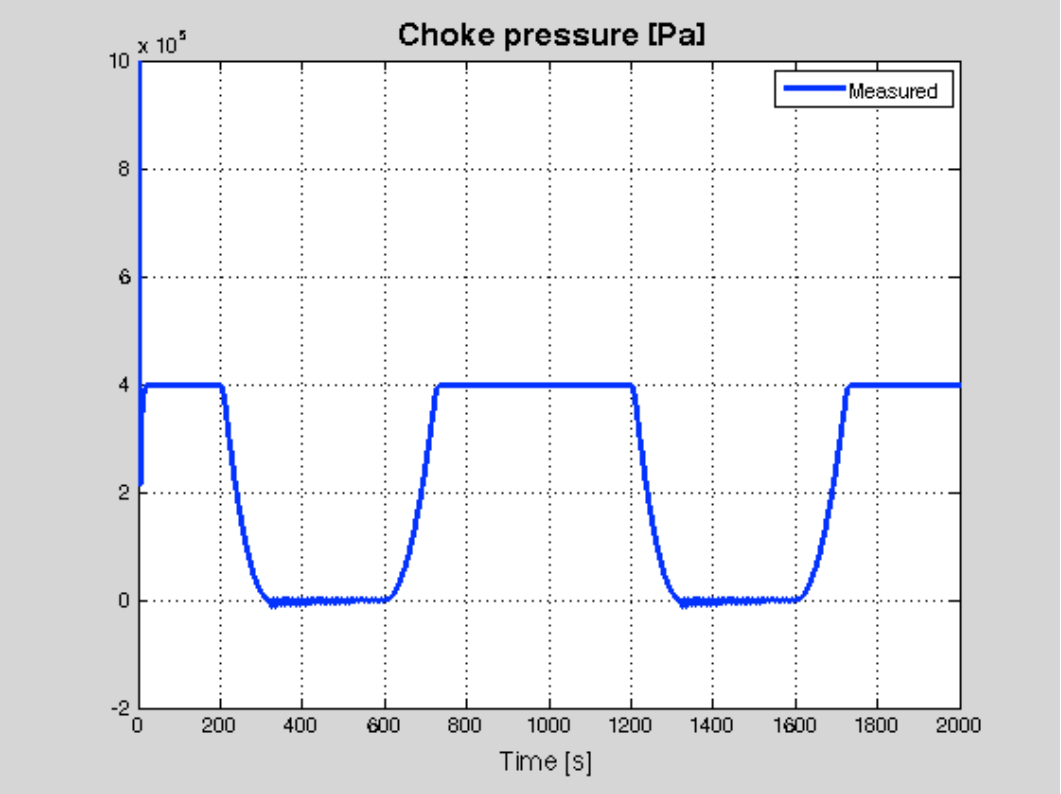

Figure 7-3. Choke pressure

As the rigpump flow rate decrease after 200 seconds we can see that the choke pressure drops as well and stabilizes around zero when the rigpump is stopped. During the connection operation there is no circulation in the well and consequently no flow through the choke. The choke pressure starts to increase after 600 seconds when the connection is made and the rigpump is ramping up. The choke pressure is stabile at 4 bar during rig pump flow rate at 2000 l/min.

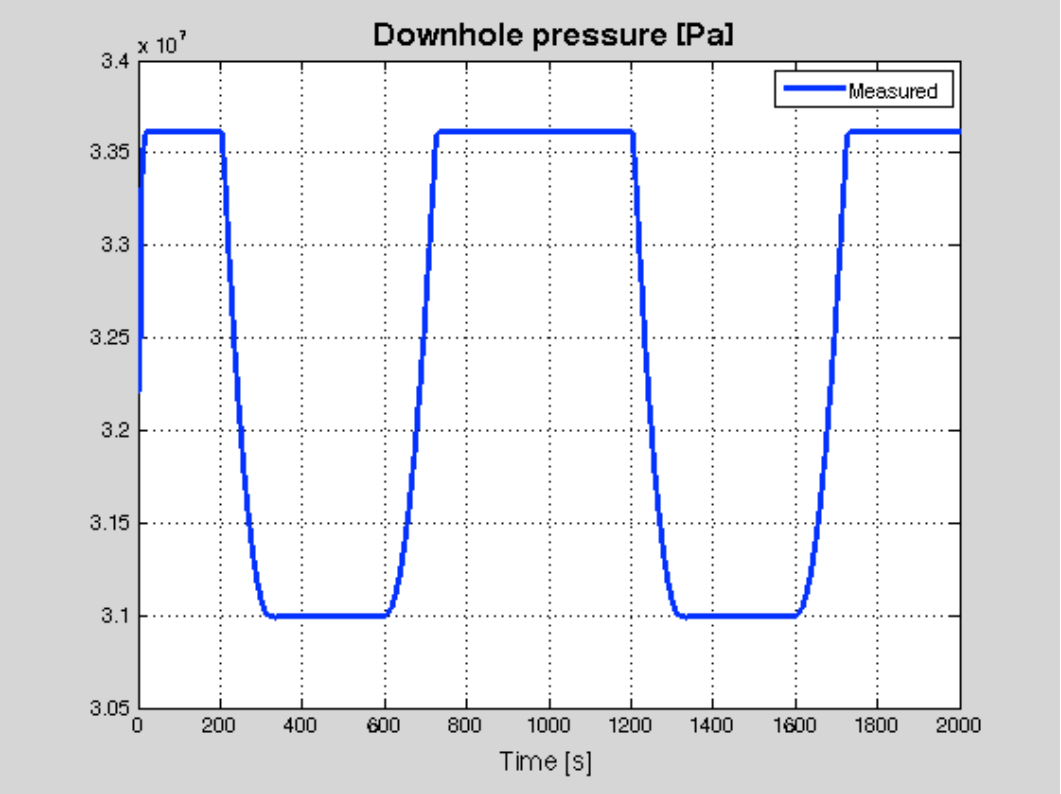

Figure 7-4. Downhole pressure

Using a mud density of 1580 kg/m^3 and the choke opening at 10% we can see that during circulation the downhole pressure is stabile at about 336 bar, but as soon as the rigpump starts ramping down so does the downhole pressure. When the rigpump stops and the mud is stationary, the figure shows that the downhole pressure has dropped over 25 bar. This is because of the frictional pressure drop experienced in the well when circulation is stopped. This pressure loss during connections is what can cause the problems described in chapter 5.

7.1.2 Example with active choke controller

In this simulation we will look at the same well as in the previous simulation, but this time with a PI controller to adjust the choke valve opening in order to achieve a more stabile BHP during connections. The PI controller is sufficient to achieve a good result in this simulation. Even though adding a derivate term to the controller would make it faster and more accurate, it would also add unnecessary complexity to the controller.

The same rigpump flow rate as in the previous simulation is used in this simulation with an active choke control.

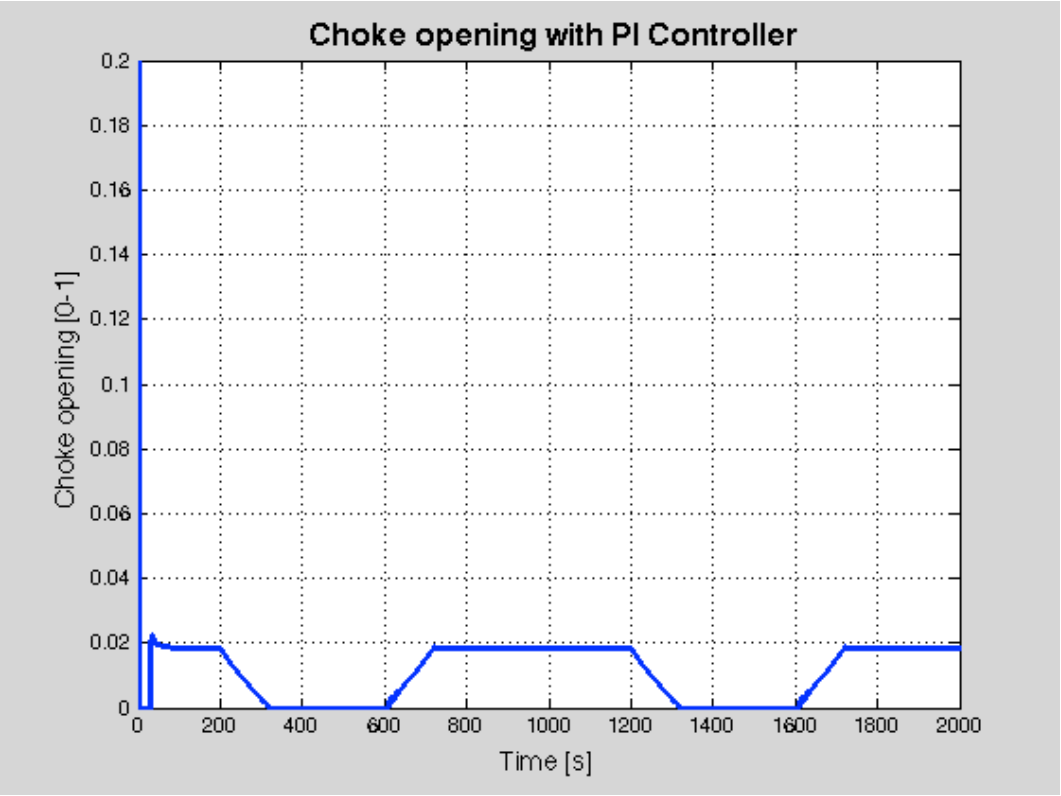

Figure 7-5. Choke opening with PI controller

As soon as the simulation starts the PI controller realizes that the downhole pressure is lower than its reference pressure of 450 bar, and closes the choke valve fully, from its initial 20% opening position, to increase the downhole pressure. After about 20 seconds the pressure surpasses the reference pressure and the choke valve is opened slightly to stabilize the pressure at 450 bar. When the connection operation starts after 200 seconds, the choke valve starts slowly closing as the rigpump flow rate is decreasing. When the rigpump starts back up

at 600 seconds, the controller recognizes this and starts opening the choke to keep the downhole pressure stabile at 450 bar.

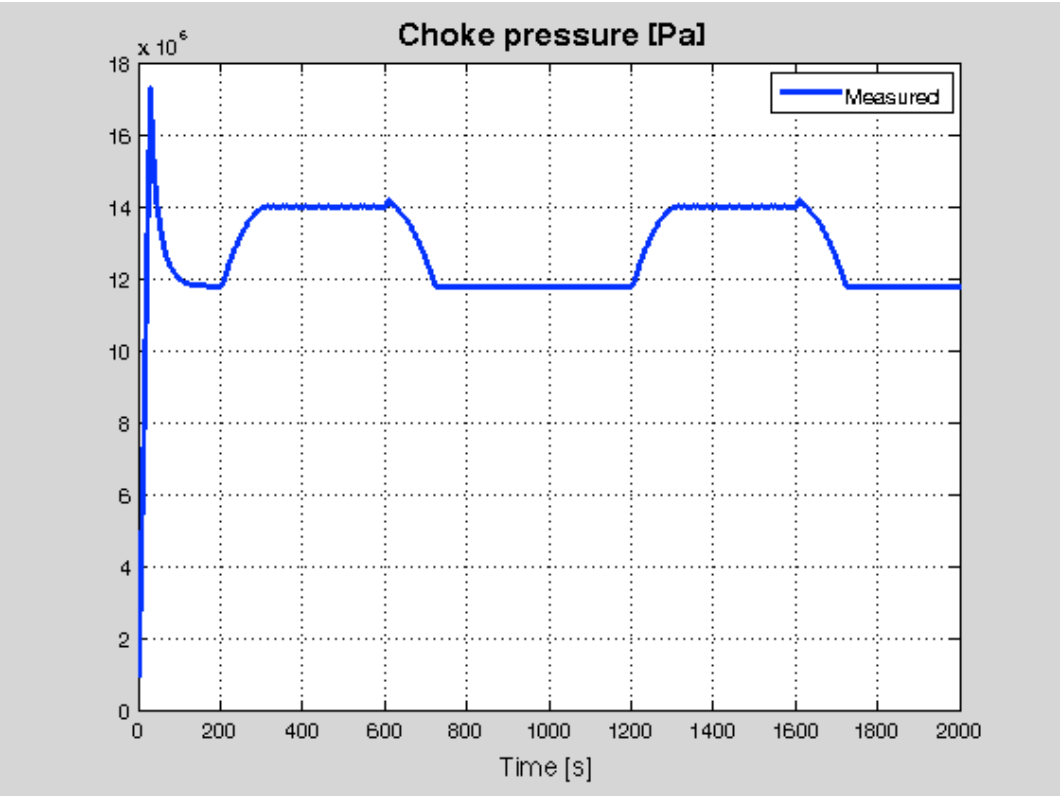

Figure 7-6. Choke pressure with PI controller

During the first seconds of the simulation, as a result of the closed choke valve and the increasing downhole pressure, the choke pressure is increasing as well. When the choke valve opens after about 20 seconds the choke pressure drops down just below 120 bar, but when the rigpump starts ramping down after 200 seconds we see that the choke pressure increasing to about 140 bar when the rigpump is stopped. This is to compensate for the 25 bar frictional pressure drop we saw in Figure 7-4.

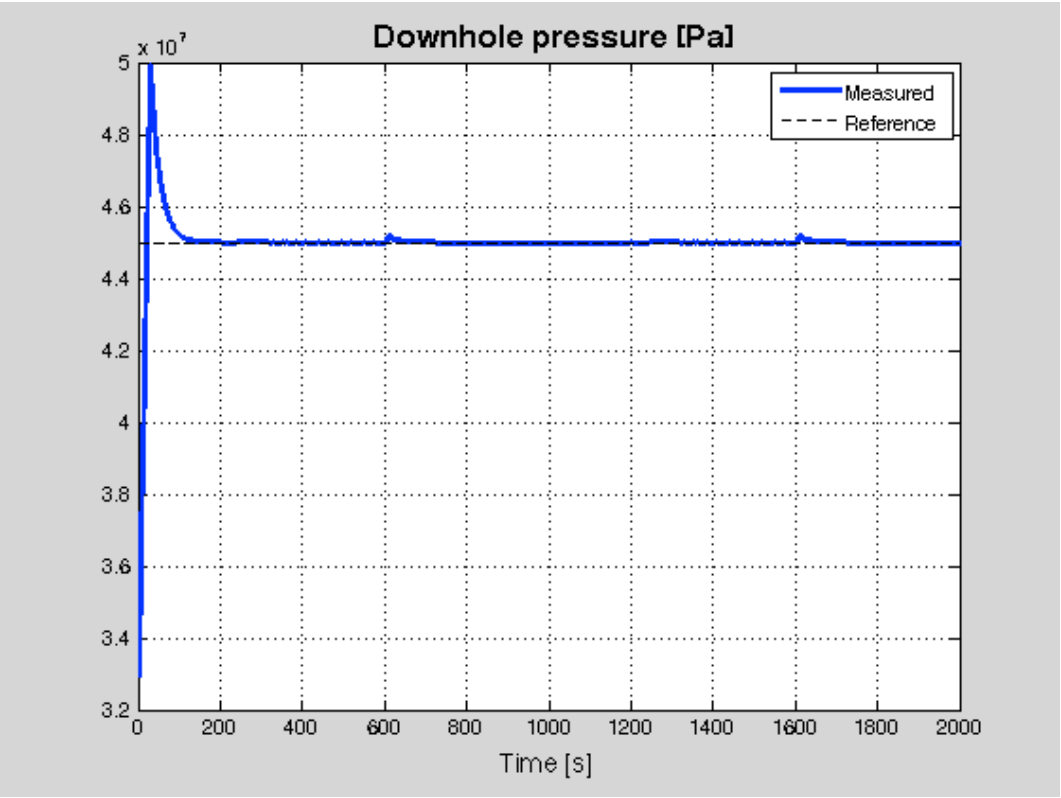

Figure 7-7. Downhole pressure with PI controller

This downhole pressure figure shows how the pressure in the well instantly starts rising when the simulation starts. The pressure exceeds the reference pressure by 50 bar before the choke valve opens and the pressure drops down to the reference pressure, 450 bar, after about 100 seconds. By adjusting the choke valve with the PI controller, the measured downhole pressure is kept stabile around the reference pressure also during the connection operations from 200 to 720 seconds and from 1200 to 1720 seconds.

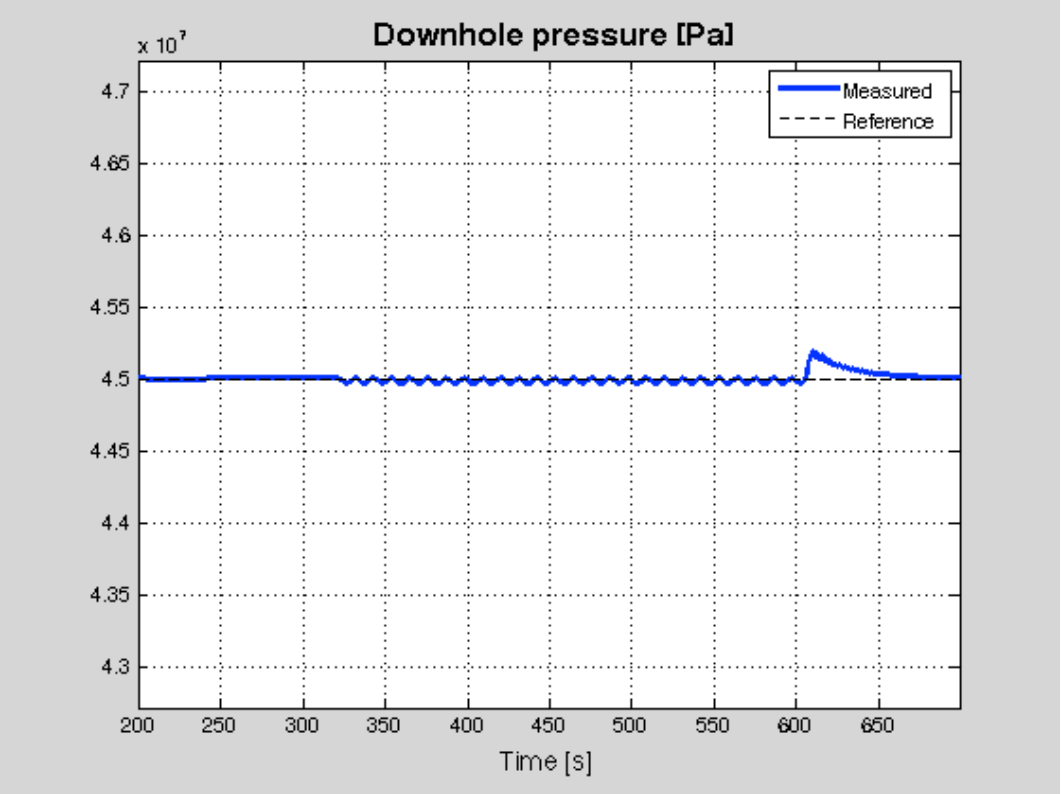

Figure 7-8. Downhole pressure (Close up)

This close up of the downhole pressure, from 200 to 700 seconds, shows how the pressure is kept steady around 450 bar during the first connection operation. There is a small peak after the rigpump starts up at 600 seconds. This peak indicates a pressure surge effect of about 2 bar over the reference pressure, which is within the industry standard for MPD systems of +/- 2,5 bar.

7.2 Kaasa model based simulations for DGD

The Kaasa model can be modified to be used for DGD. Instead of applying backpressure using a choke valve, the backpressure is applied using the mud level in the riser. The control algorithms are similar to controlling the downhole pressure with the MPD system in the previous subchapter. To modify the Kaasa model to be used with DGD, the dynamics of flow rate through bit is modified by adding the p_{rb} parameter like this

$$\dot{q}_b = \frac{1}{M}\left(p_p\left(p_c + p_{rb}\right)\right) - \left(F_d + F_b + F_a\right)q_b^2 + \left(\rho_d - \rho_a\right)gh$$

7.2.1 Benchmark simulation

The DGD system in these simulations are based on the controlled mud level system where a topfill pump, in conjunction with a subsea pump, is used to increase the level of mud in the riser. A PI controller is used to control the flowrate of the subsea pump.The topfill fluid is lighter than the drilling mud and is equivalent to water, at 1000 kg/m^3. The flow rate through the topfill pump is kept constant at 2000 l/min.

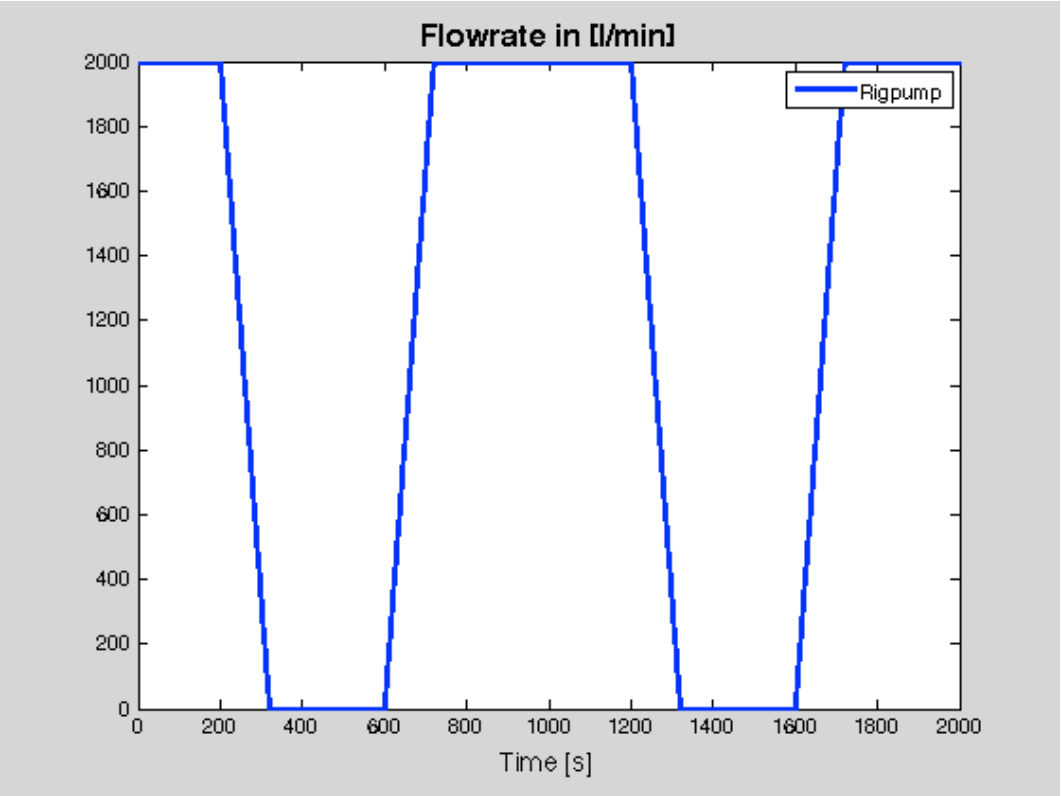

Figure 7-9. Flow rate from rigpump

The simulations in this subchapter will all be using the same rigpump flow rate scenario, illustrating two connection operations, as in the previous subchapter.

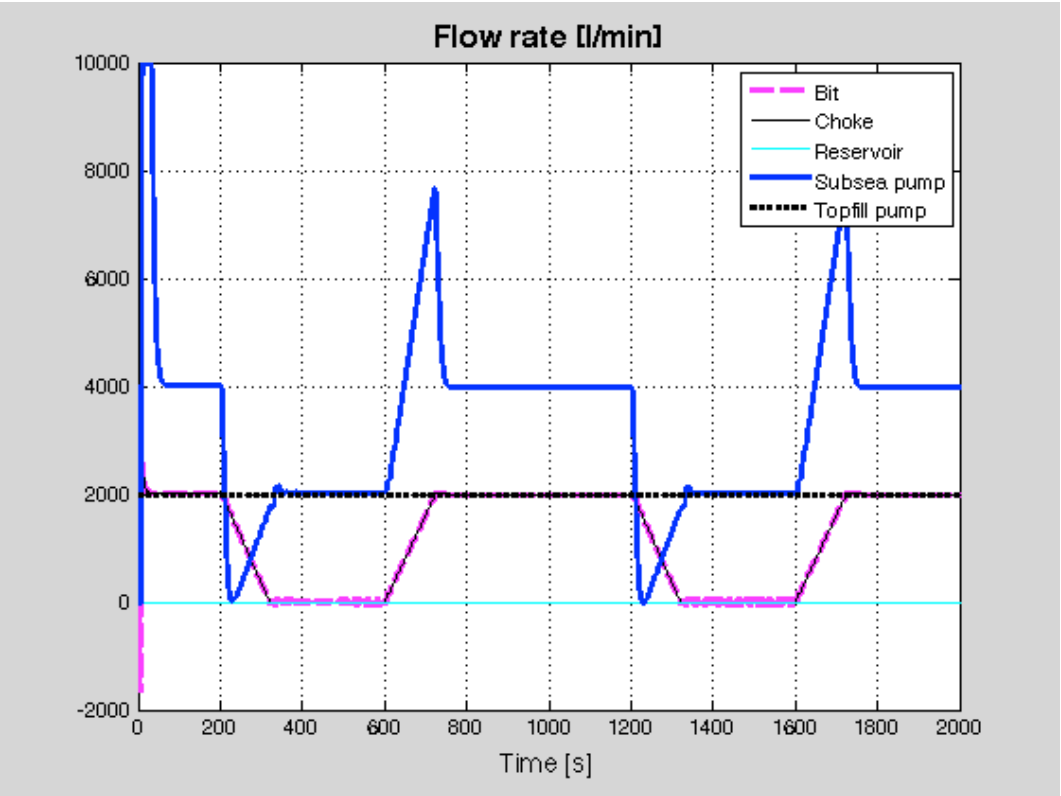

Figure 7-10. Flow rate (benchmark)

This figure show the flow rates through the different parts of the well. We can see that as soon as the simulation starts, the subsea pump, controlled by the PI controller, is ramped up to its maximum capacity of 10000 l/min in order to lower the mud level in the riser from the initial level at 600 m. This in turn lowers the downhole pressure. When the downhole pressure reaches its reference value at 450 bar, the subsea pump stabilizes at 4000 l/min, which is the sum of the flow rate from the rigpump and the topfill pump. At this point the flow into the well is equal to the flow out and the riser level is kept relatively stabile at about 340 m above the subsea pump as seen in Figure 7-11. The rest of the riser is filled with the lighter topfill mud.

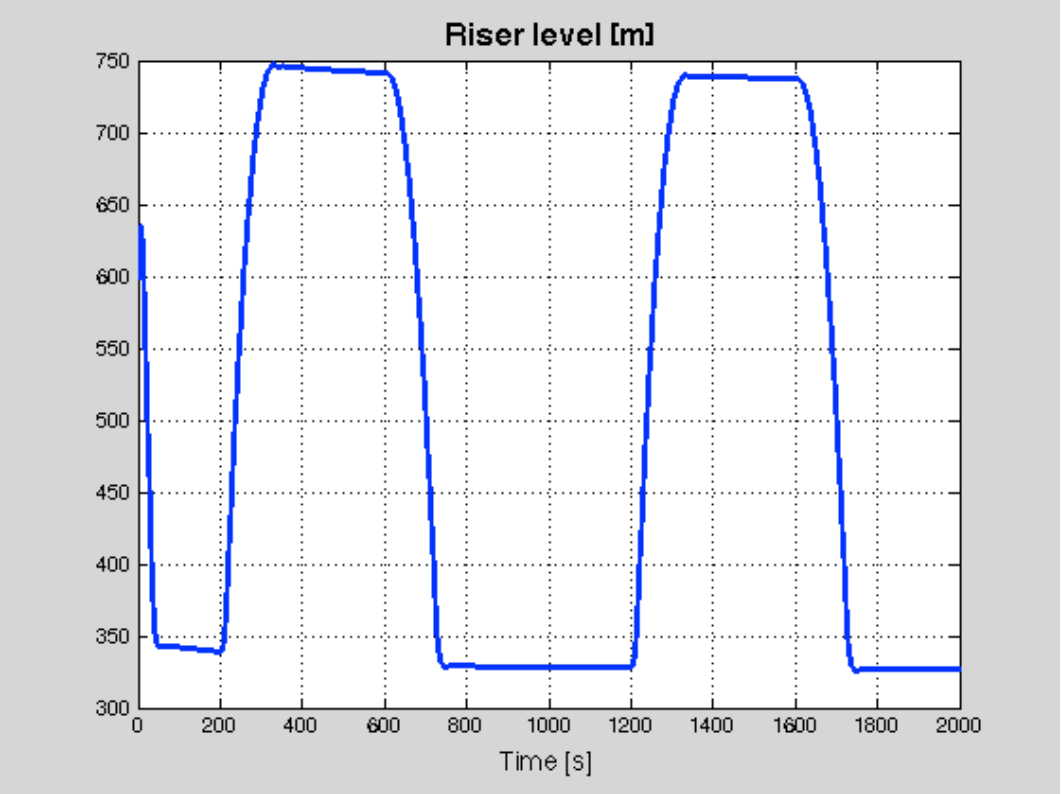

Figure 7-11. Riser level (benchmark)

At 200 seconds, when the rigpump starts ramping down, the subsea pump flow rate drops to zero. This allows the riser mud level to increase, in order to compensate for the frictional pressure drop, and the downhole pressure to stay around 450 bar. As the rigpump flow rate is decreasing towards zero, the flow rate through the subsea pump is increasing. When the rigpump is stopped after 320 seconds the subsea pump is pumping 2000 l/min out of the riser, the same amount as the topfill pump is pumping into the riser and the riser level is relatively stabile just under 750 m.

The subsea pump flow rate is ramped up when the rigpump starts up after the connection. This lowers the riser level back down to around 330 m and the downhole pressure is still at 450 bar.

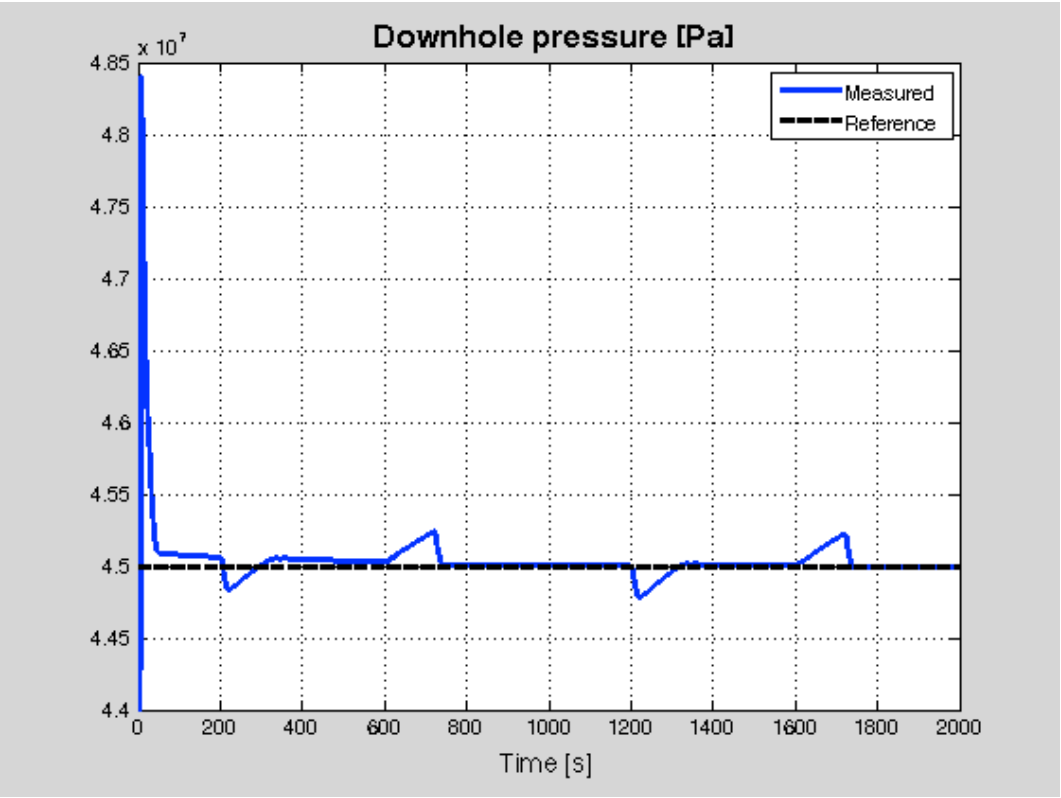

Figure 7-12. Downhole pressure (benchmark)

As we can see from the downhole pressure figure, the PI controller regulates the subsea pump so that the reference downhole pressure is reached in under 50 seconds. This is about half the time it took in the MPD simulation with choke control, where the reference pressure was reached after around 100 seconds. We can also see that the surge and swab effects, when using the DGD system, are slightly bigger compared to the MPD simulation with active choke controller. This indicates that the MPD system can react to changes faster than the DGD system is able to. Still, with the DGD system, the downhole pressure is kept within the +/- 2,5 bar industry standard during connections.

7.2.2 Increased topfill fluid density

In this simulation we will increase the density of the topfill fluid and review the effect this has during the connection operation. The rig pump flow rate will be the same as in the previous simulations. Topfill fluid density is increased to 1100kg/m^3.

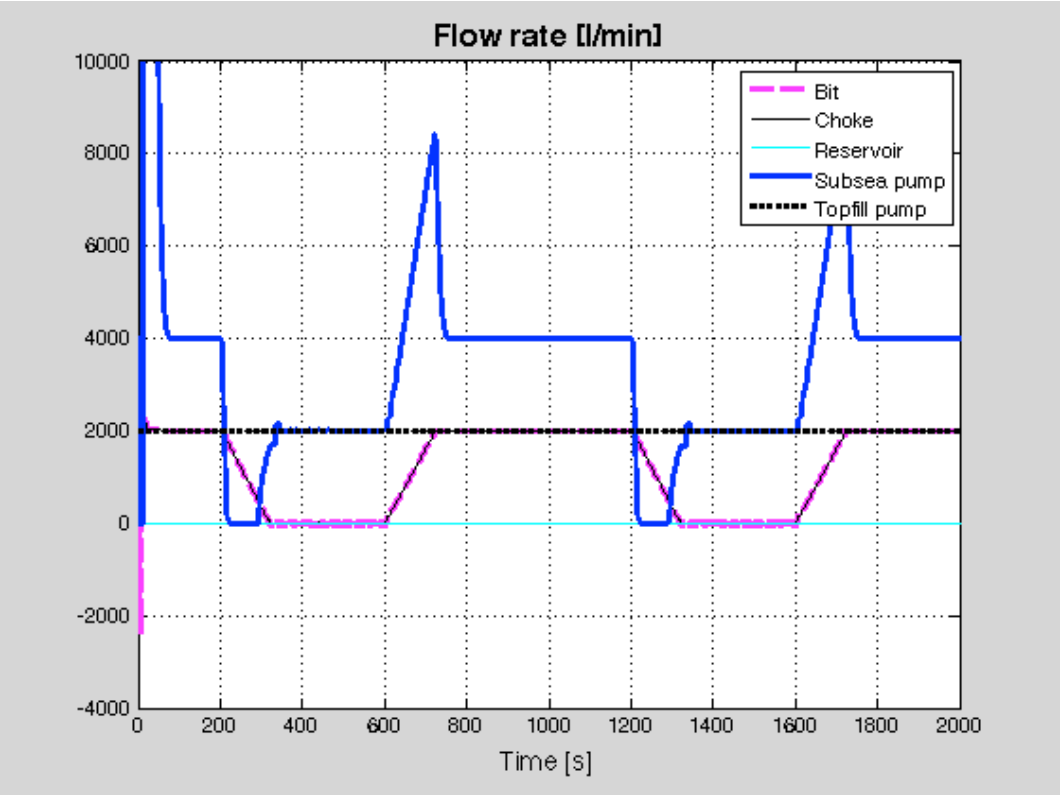

Figure 7-13. Flow rate (Increased topfill fluid density)

If we compare the behavior of the subsea pump in this simulation and the last we can see that when using a heavier topfill fluid, the subsea pump, at the start of the simulation, stays at maximum capacity for a longer time period than in the first DGD simulation. This allows the riser level to drop all the way down to 200 m. The riser level needs top drop that low because of the added pressure contribution from the heavier topfill mud in the upper part of the riser.

The figure also shows that once the connection operation starts, at 200 seconds, the subsea pump is shut down for almost 100 seconds. This is needed in order to raise the riser level from 200 m up to almost 700 m once the rigpump stops and the frictional pressure is lost.

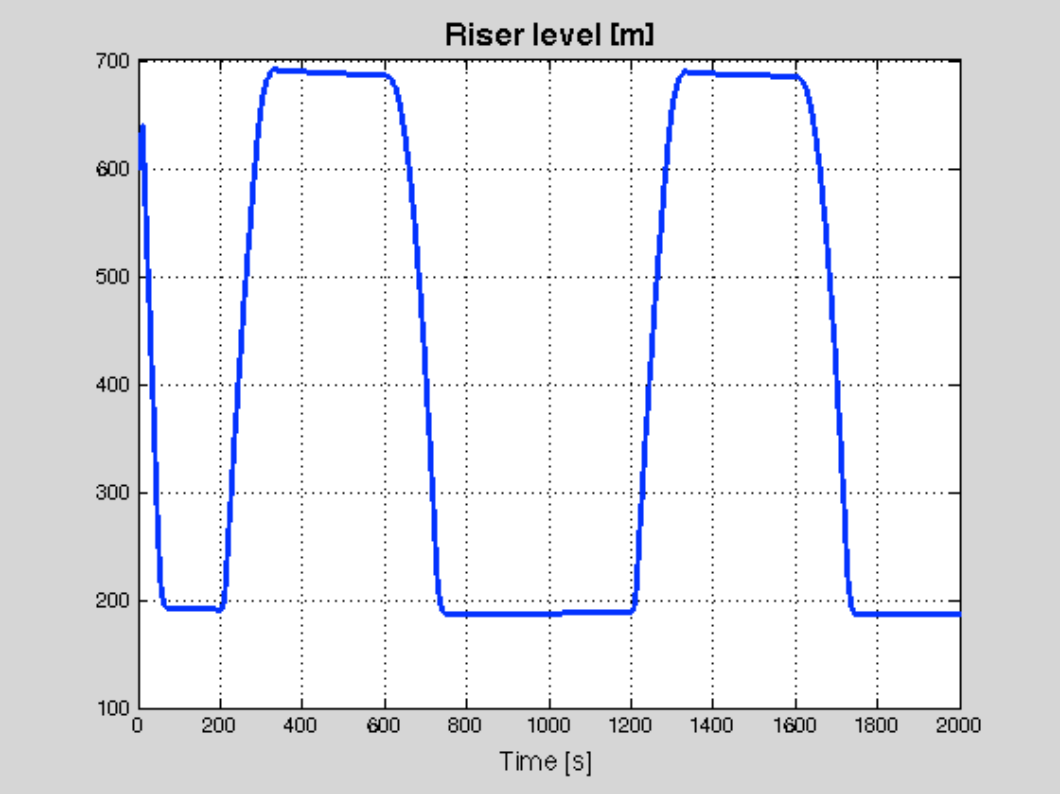

Figure 7-14. Riser level (Increased topfill fluid density)

With the heavier top fill fluid density, the riser level is stabile at just under 200 m during circulation. When circulation is stopped, the riser mud level has to be raised 500 m to compensate for the frictional pressure loss.

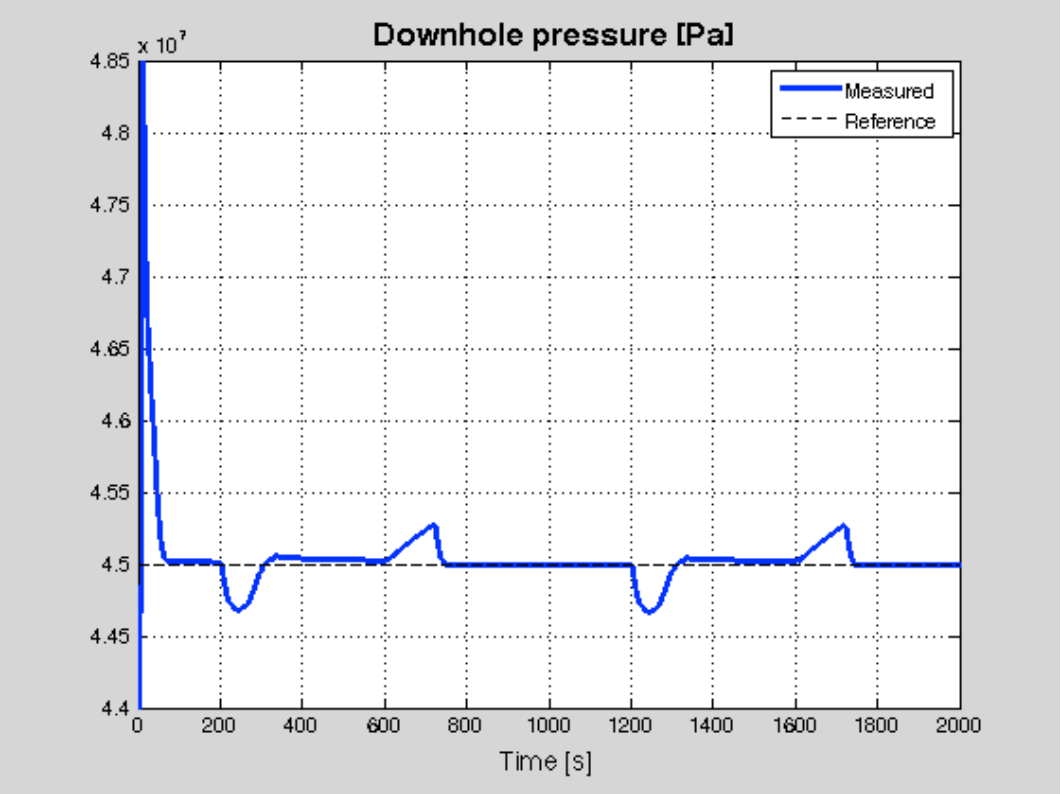

Figure 7-15. Downhole pressure (Increased topfill fluid density)

Compared to the previous simulation, where the reference downhole pressure was reached after less than 50 seconds, this simulation is slightly slower. This is due to the fact that the riser level has to be changed by 500 m from the steady level during circulation to the new steady level when circulation is stopped. With a topfill fluid density higher than 1100 kg/m^3 the pressure change would be even slower. The simulation also shows a slight increase in the size of the surge and swab effect of the connection procedure, but the pressure deviations are still within the industry standard.

7.2.3 Lowered topfill fluid density

Again we are using the same connection operation flow rates as seen in the previous simulations. Topfill fluid density is now lowered to 800kg/m^3.

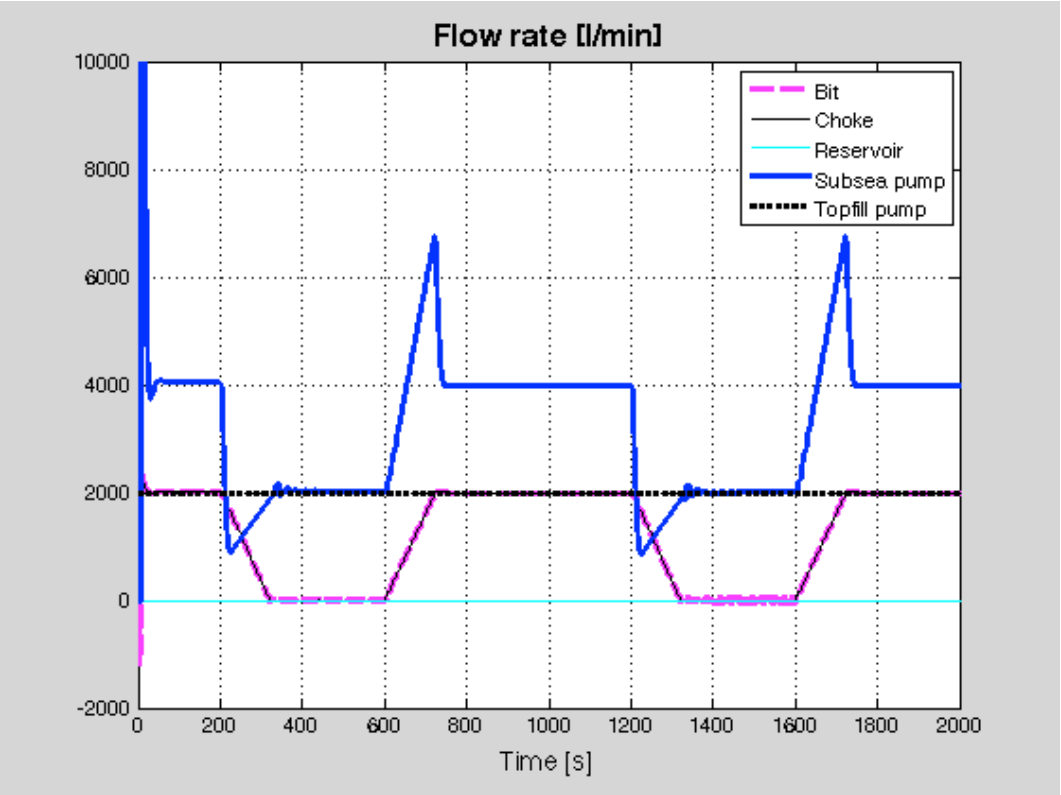

Figure 7-16. Flow rate (lowered topfill fluid density)

The flow rate figure is showing that the subsea pump does not stay at maximum capacity for as long as it did in the previous simulation. The flow rate drops quickly down to 4000 l/min, where $q_{in,riser} = q_{out,riser}$. When the connection operation starts, the subsea pump flow rate drops only down to about 1000 l/min and not all the way down to zero like in the previous simulations. The reason for this is that the difference between riser level during circulation and when circulation is stopped, is lower than in the previous simulation with increased topfill fluid density.

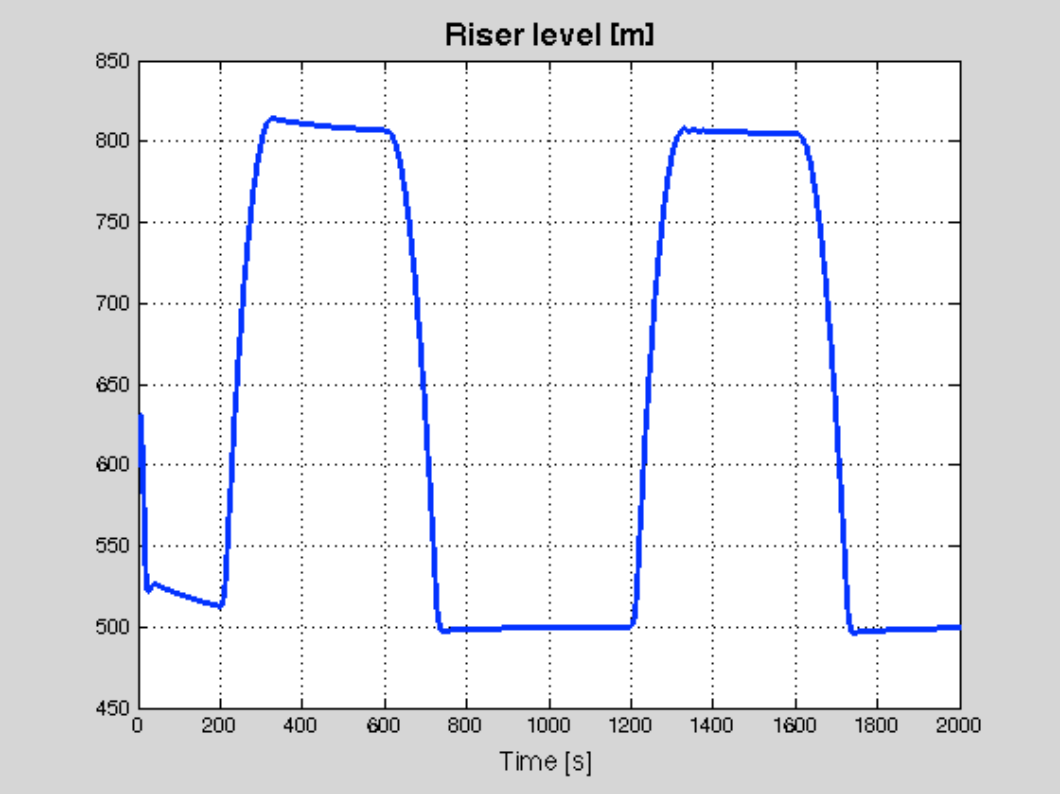

Figure 7-17. Riser level (lowered topfill fluid density)

The riser level figure indicates that, with the 450 bar reference downhole pressure, the steady riser level is at about 500 m during circulation. This level drop is smaller compared to the drop we saw with a higher density topfill fluid. This shorter drop from the initial riser height is the reason why the subsea pump stays at maximum capacity for such a short time.

The figure is also saying the when circulation is being ramped down, the riser level needs to be raised by about 300 m compared to 500 m in the last simulation. This is because of the reduced pressure contribution from the lighter topfill fluid.

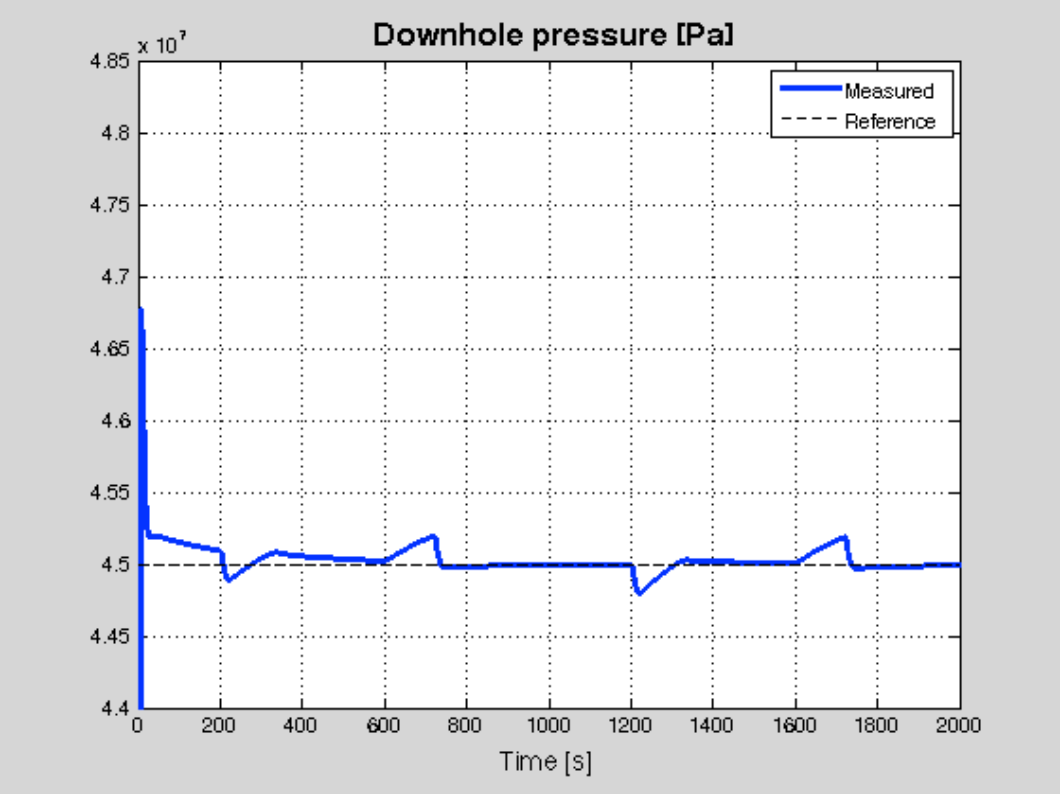

Figure 7-18. Downhole pressure (lowered topfill fluid density)

As a result of using a lower topfill fluid density we see that the downhole pressure is within +/- 2,5 bar of the reference value after only 20 seconds. The downhole pressure figure also shows that the effects of surge and swab are low and well within the limit.

7.2.4 Increased topfill flow rate

To review what happens when the flow rate into the riser is increased we will now raise the topfill flow rate to 3000 l/min. All other parameters are just as in the benchmark simulation in subchapter 7.2.1.

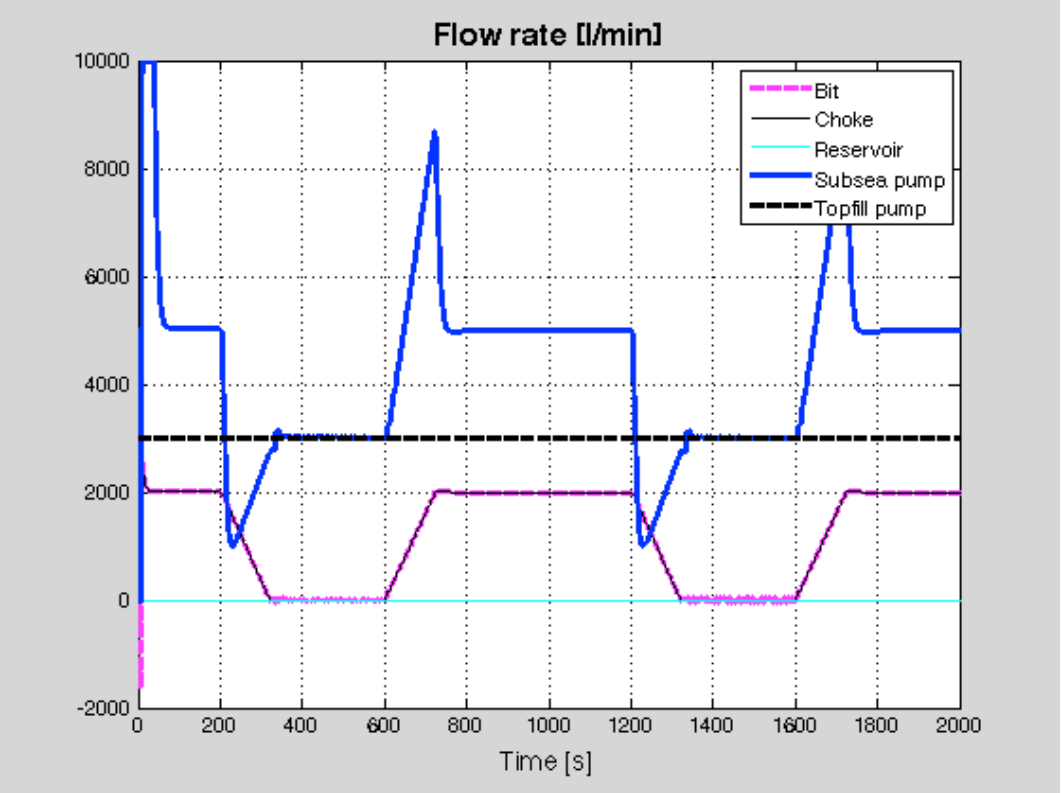

Figure 7-19. Flow rate (increased topfill flowrate)

We can see from the flow rate figure that it has the same shape as in the benchmark simulation. The difference is that the subsea pump flow rate has been shifted up to compensate for the increased topfill pump flow rate. During circulation the flow rate into the riser is composed of the rigpump (2000 l/min) and the topfill pump (3000 l/min). The PI controller adjusts the subsea pump flow rate according to the flow rate into the riser and sets the subsea pump at 5000 l/min to maintain a constant riser level and a constant downhole pressure.

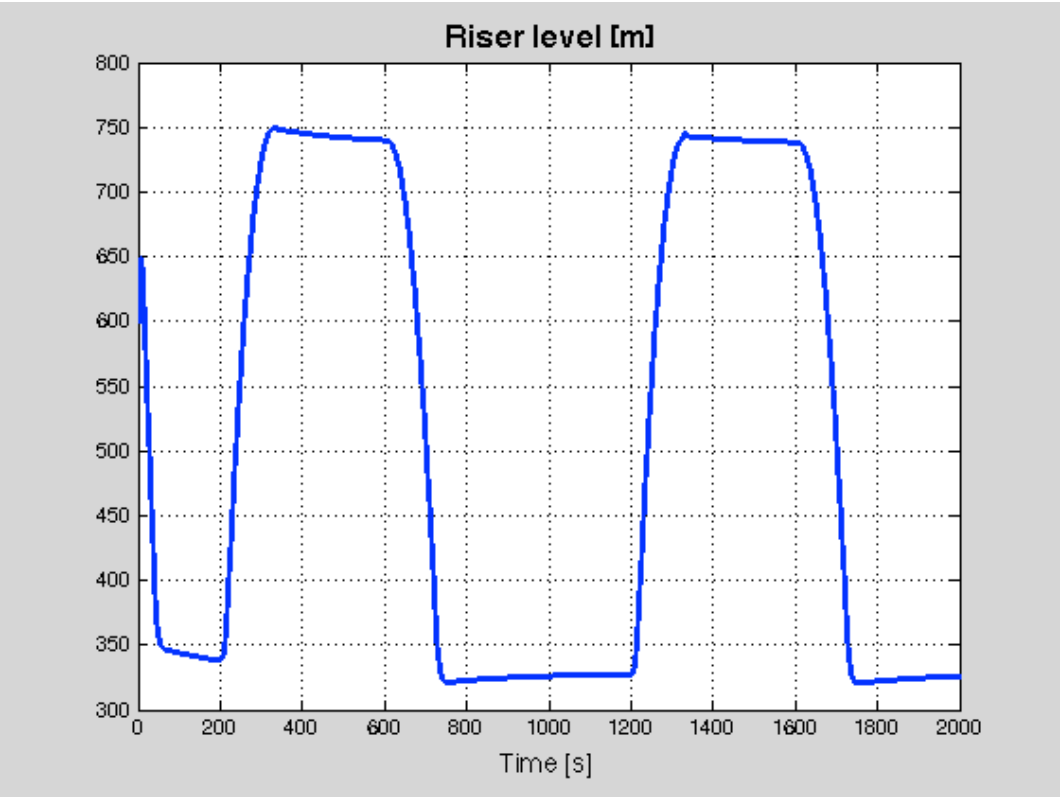

Figure 7-20. Riser level (increased topfill flow rate)

Because the density of the topfill fluid is still at 1000 kg/m^3 we can see little or no changes in the riser level. The riser level in this simulation is also stabile at just under 750 m when circulation is stopped, and below 350 m during circulation. This is similar to the benchmark simulation.

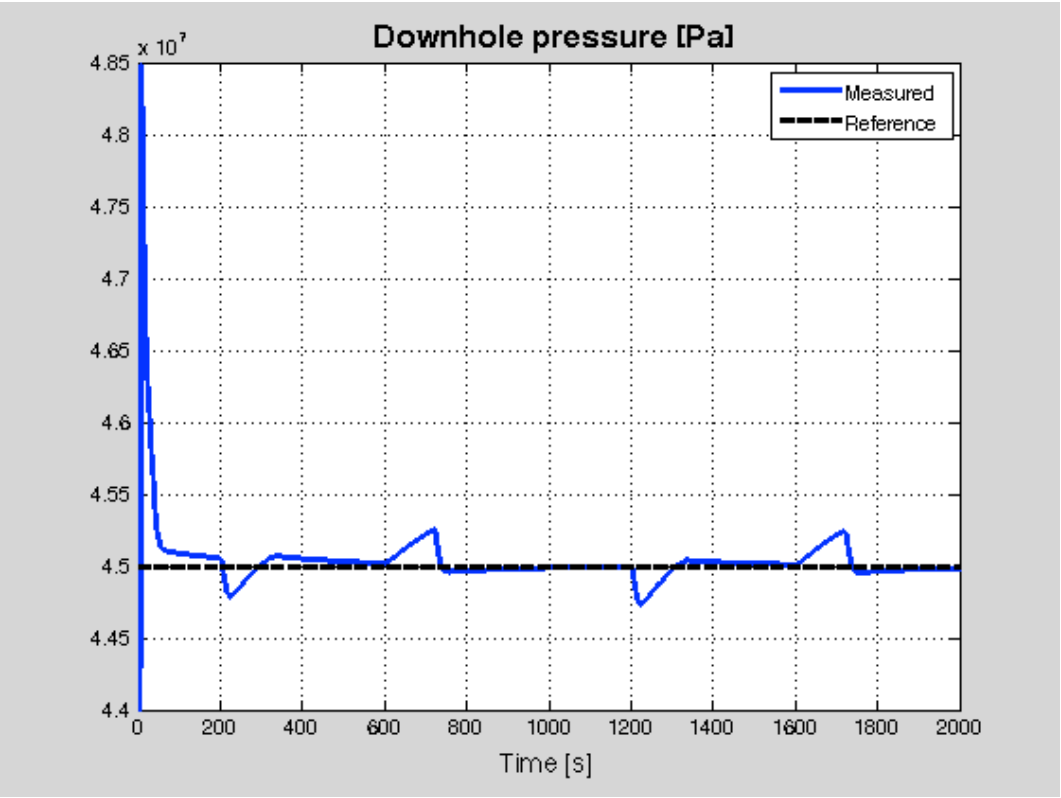

Figure 7-21. Downhole pressure (increased topfill flow rate)

Because the subsea pump compensates for the increase in topfill flow rate, there is very little difference in the downhole pressure compared to the benchmark simulation.

7.2.5 Lowered topfill flow rate

This simulation will show if a lowered topfill flow rate has any effect on the pressure in the well. The topfill flow rate will now be set to 1000 l/min. All other parameters are just as in the benchmark simulation in subchapter 7.2.1.

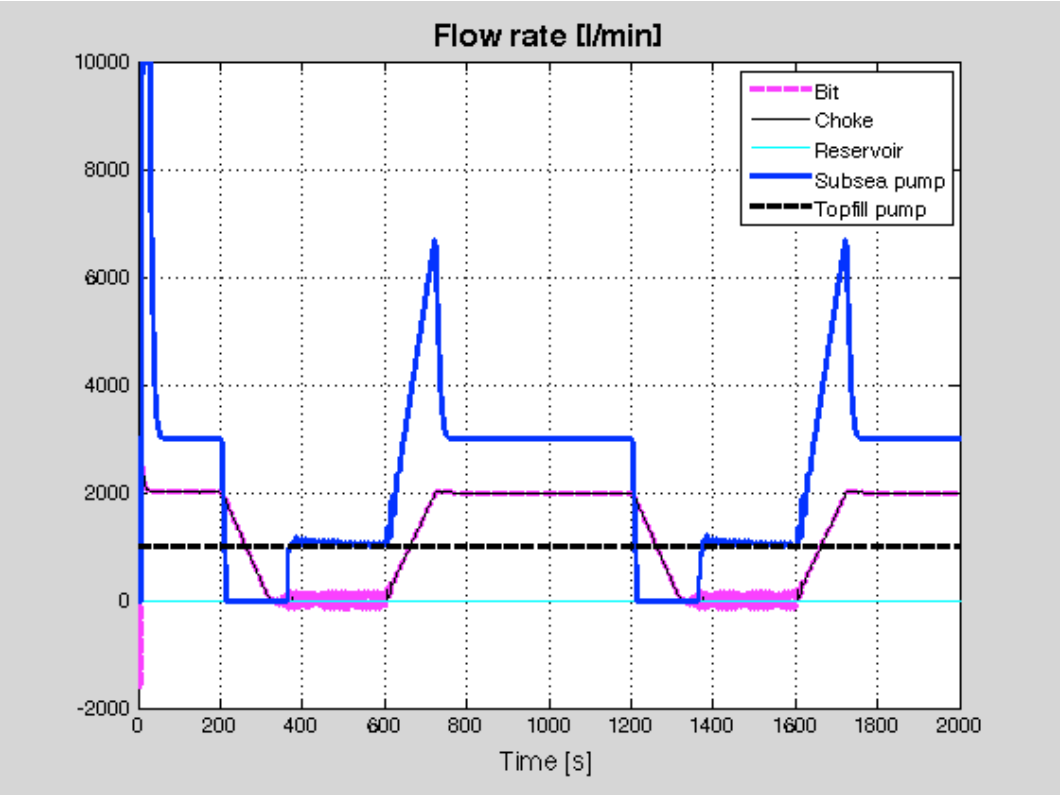

Figure 7-22. Flow rate (lowered topfill flow rate)

The decreased topfill flow rate has a significant impact on the behavior of the subsea pump. When the connection operation starts at 200 seconds the subsea pump shuts down and stays off for about 150 seconds. The reason for this is that it takes longer to fill up the riser when the flow rate from the topfill pump is set at only 1000 l/min. The subsea pump starts about 30 seconds after the rigpump circulation has stopped.

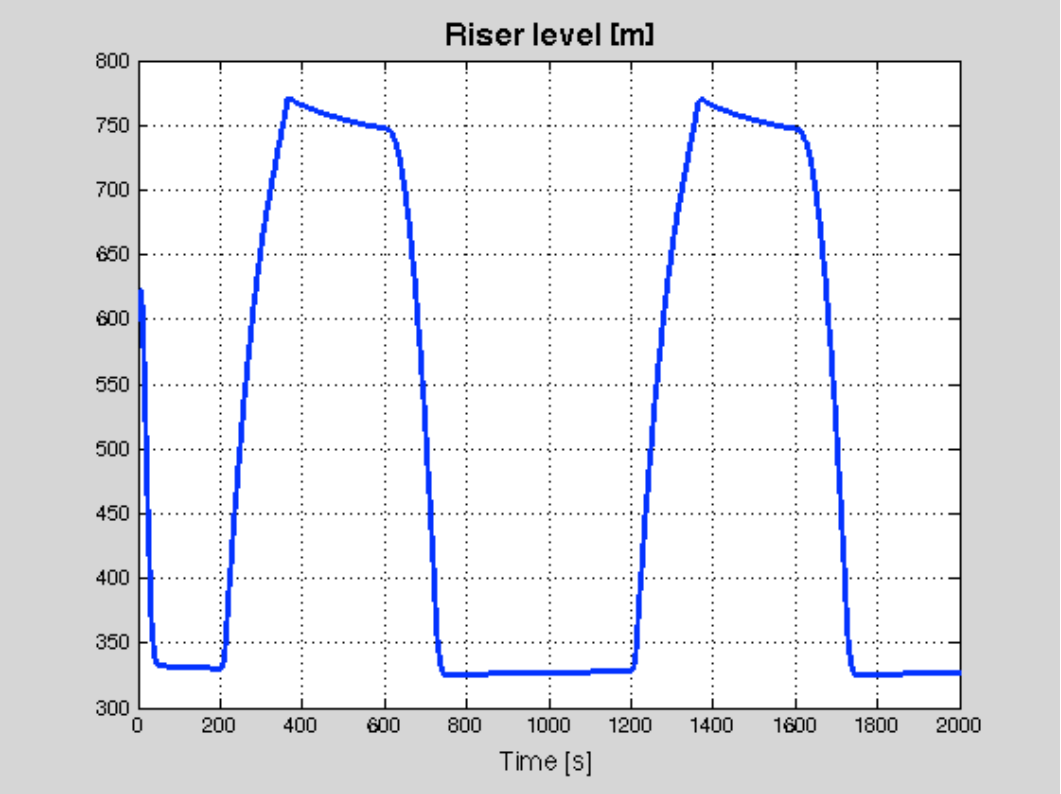

Figure 7-23. Riser level (lowered topfill flow rate)

With the lower topfill flowrate, it takes a bit longer to fill up the riser to the necessary level compared to the benchmark simulation. While the benchmark simulation filled up the riser at around the 730 second mark, in this simulation the required riser level is met at around 765 seconds.

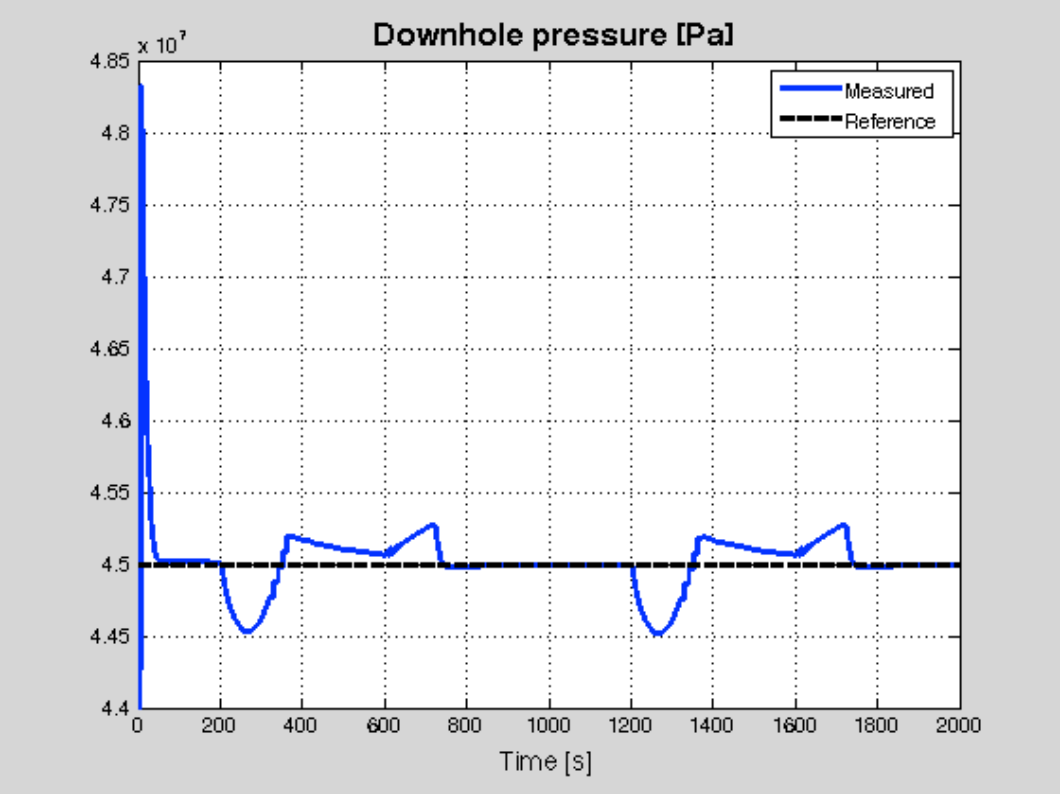

Figure 7-14. Downhole pressure (lowered topfill flow rate)

With a lowered topfill flowrate we can see that the response of the system is reduced. This can be seen in the swab effect experienced right after the connection operation starts. The system is also slower to recover from the pressure drop compared to the benchmark simulation. The swab effect is this simulation is almost 5 bar and not within the industry standard, but this may not be a problem if the drilling window can allow it.

8 Conclusion

As offshore wells are being drilled in more and more hostile environments, the need for new drilling technology is increasing. The literature study done is this thesis shows that DGD might very well be the technology the industry is looking for. The DGD system is capable of:

- Reducing well cost with up top 50% by reducing NPT and the number of casing strings needed to reach TD.
- Widen the drilling window
- Eliminate pump and dump practice
- Better kick detection
- Reducing challenges associated with connection operations

Because DGD is a new an unconventional drilling technology, it also has its share of challenges. Perhaps the most difficult challenge to overcome is convincing a conservative industry that DGD can be of great help when drilling difficult prospects such as deepwater reservoirs and depleted reservoirs.

This thesis presents a method for modeling DGD operations using Kaasa's modell focusing on comparing DGD and MPD with regards to downhole pressure during conection operations. Special emphasis was placed on the variables related to the topfill pump.

The simulations showed that the DGD system could reach the reference downhole pressure in nearly half the time compared to a regular MPD system. This is important with regards to reducing the exposure time of uncased formation to high pressures. We can also see that the surge and swab effects, when using the DGD system, are slightly bigger compared to the MPD simulation with active choke controller. This indicates that the MPD system is able to react to changes quicker than the DGD system is able to.

From the simulation with lowered topfill fluid density we saw that a lower fluid in the upper part of the riser can improve the response of the system, as this simulation was the fastest to reach the reference downhole pressure. This simulation was also quick to recover from surge and swab effects. Further simulations could include changes to the riser height, i.e., the water depth and adding a booster pump to increase riser level change speed and system response.

9 Bibliography

Brown, J., Urvant, V., Thorogood, J., & Rolland, N. L. (2007, 04 23). *More Driling and Production: Oil & Gas Journal*. Retrieved April 06, 2014, from Oil & Gas Journal: http://www.ogj.com/articles/print/volume-105/issue-16/drilling-production/special-report-sakhalin-rmr-1-elvary-neftegaz-plans-riserless-system-for-sakhalin-drilling-program.html

Dowell, D. (2011). Dual Gradient Drilling - The System. *DEA Presentation* (p. 40). Chevron North America Exploration and Production Company.

Dowell, J. D. (2010). *Deploying the World's First Commercial Dual Gradient Drilling System.* Society of Petroleum Engineers. Galveston,Texas: SPE 137319.

Drilling Contractor. (2011, May 10). *News: Drilling Contractor*. Retrieved April 04, 2014, from Drilling Contractor: http:// www.drillingcontractor.org/dual-gradient-drilling-differentiators-benefits-barriers-to-implementation-9533

Enhanced Drilling. (n.d.). *Solutions: RMR - Riserless Mud Recovery: Enhanced Drilling*. Retrieved April 04, 2014, from Enhanced Drilling: http://www.enhanced-drilling.com/solutions/rmr-riserless-mud-recovery

Fossli, B., & Sangesland, S. (2006). *Controlled Mud-Cap Drilling for Subsea Applications: Well-Control Challenges in Deep Waters.* Society of Petroleum Engineers. Houston: SPE 91633.

Fossli, B., & Stave, R. (2014). *Drilling Depleted Reservoirs using Controlled Mud Level Technology in Mature Subsea Fields.* Bergen: SPE 169178.

Gaup, T. H. (2012). *Simulations of Dual Gradient Drilling.* Norwegian University of Science and Technology, Petroleum Engineering and Applied Geophysics. Trondheim: NTNU.

Güyagüler, B., Papadopoulos, A., & Philpot, J. (2009). *Feedback Controllers for the Simulation of Field Processes.* The Woodlands: SPE 118969.

Ghiselin, D. (2012, July 01). *More Drilling & Completion News: Offshore Magazine*. Retrieved March 23, 2014, from Offshore Magazine: http://www.offshore-mag.com/articles/print/volume-72/issue-7/drilling-and-completion/dual-gradient-technology-expands-deepwater-drilling-opportunities.html

Haj, A. M. (2012). *Dual gradient drilling and use of the AUSMV scheme for investigating the dynamics of the system.* University of Stavanger, Department of Petroleum Engineering. Stavanger: UiS.

Herrmann, R., & Shaughnessy, J. (2001). *Two Methods for Achieving a Dual Gradient in Deepwater.* Amsterdam: SPE/IADC 67745.

Hsieh, L., & Scott, K. (2012, March 27). *News: Drilling Contractor*. Retrieved March 10, 2014, from Drilling Contractor: http://www.drillingcontractor.org/the-essentials-of-dual-gradient-drilling-several-variations-under-development-15014

IADC. (2011). *UBO & MPD Glossary.* Retrieved 04 16, 2014, from International Association of Drilling Contractors: www.iadc.org

Kaasa, G., Stamnes, O., Imsland, L., & Aamo, O. (2011). *Intelligent Estimation of Downhole Pressure Using a Simple Hydraulic Model.* Denver: SPE 143097.

Mazerov, K. (2012, March 27). *News: Drilling Contractor*. Retrieved March 15, 2014, from Drilling Contractor Web Site: http://www.drillingcontractor.org/successful-dual-gradient-system-follows-natures-pressure-profiles-15044

Mazerov, K. (2012, March 27). *News: Drilling Contractor*. Retrieved 06 06, 2014, from Drilling Contractor: http://www.drillingcontractor.org/successful-dual-gradient-system-follows-natures-pressure-profiles-15044

Maris. (2009, July). *Download CCS Benefits Document: Maris.* Retrieved June 1, 2014, from Maris: http://maris-eu.com/Downloads/CCD_doc.pdf

MCS Kenny. (2013). *Final Report 03-Kick Detection and Associated Technologies.* Houston: MCS Kenny.

Nygaard, G. (2014, April 03). Drilling Automation - PET525 - Control algorithms II. Stavanger, Rogaland, Norway: UiS.

Nygaard, G., & Godhavn, J.-M. (2013). *Automated Drilling Operations* . Stavanger, Rogaland, Norway: University of Stavanger.

Rajabi, M. M., Rohde, B., Maguire, N., Stave, R., & Tapper, R. (2012). *Successful Implementations of Tophole Managed Pressure Cementing and Managed Pressure Drilling in the Caspian Sea.* Milan: SPE 156889.

Rajabi, M. M., Toftevåg, K., Stave, R., & Ziegler, R. (2012). First Application of EC-Drill in Ultra-Deepwater - Proven Subsea Managed Pressure Drilling Method. *SPE Deepwater Drilling and Completions Conference* (p. 12). Galveston: SPE 151100.

Rezk, R. (2013). *Safe and Clean Marine Drilling with Implementation of "Riserless Mud Recovery Technology - RMR".* Moscow: SPE 166839.

Saeed, S., Lovorn, R., & Knudsen, K. A. (2012). *Automated Drilling Systems for MPD—The Reality.* San Diego: SPE 151416.

Schubert, J., Juvkam-Wold, H., & Choe, J. (2006). *Well-Control Procedures for Dual-Gradient Drilling as Compared to Conventional Riser Drilling.* Society of Petroleum Engineers. SPE 99029.

Sigurjonsson, K. Ö. (2012). *Dual gradient drilling simulations.* Norwegian University of Science and Technology, Petroleum Engineering and Applied Geophysics. Trondheim: NTNU.

Smuts, J. (2011, 01 17). *A Tutorial on Feedforward Control: Control Notes*. Retrieved May 19, 2014, from Control Notes - Reflections of a Process Control Practitioner: http://blog.opticontrols.com/archives/297

Smith, D., Winters, W., Tarr, B., Ziegler, R., Riza, I., & Faisal, M. (2010). *Deepwater Riserless Mud Return System for Dual Gradient Tophole Drilling.* Kuala Lumpur: SPE 130308.

Smith, K., Gault, A., Witt, D., & Weddle, C. (2001). *SubSea MudLift Drilling Joint Industry Project: Delivering Dual Gradient Drilling Technology to Industry.* New Orleans: SPE 71357.

Smith, K., Gault, A., Witt, D., Botros, F., Peterman, C., Tangedahl, M., et al. (1999). *Magazine: World Oil ONLINE*. Retrieved March 25, 2014, from World Oil ONLINE: http://www.worldoil.com/August-1999-SubSea-MudLift-Drilling-JIP-Achieving-dual-gradient-technology.html

Statoil. (2013). Dual Gradient Drilling - Gas in riser mitigation actions . (p. 10). Statoil.

Statoil. (2014). Dual Gradient Drilling (DGD). *UiS Info* (p. 29). Statoil.

Østvik, T. (2011). *Dual Gradient Drilling.* Stavanger: UiS.

10 Appendix

The MATLAB scripts used in this thesis are will be presented here.

10.1 Tank example without controller

```
clear all; clc;

Ts=1;
Tf=2000;

qinn = 0.2;% [m3/s]
h=0.7;
A=10;
rho=1620;
Kc=0.14;
g=9.81;
z=1;  %Valve opening
delta_z=0;
harray =[];
qin_array =[];
qout_array =[];
qut=z*Kc*sqrt(g*h);



for i=1:Ts:Tf

    %change flow rate in
    if (i >= 500) && (i < (500)+60)
      qinn = qinn+0.001666667;% [m3/s] (ramp up to 0.3 m3/s in one minute)
    end


    if (i >= 1000) && (i < (1000)+60)
      qinn = qinn-0.001666667;% [m3/s] (ramp down to 0.2 m3/s in one
minute)
    end

    %simulate
    deltah=(1/A)*(qinn-qut);
    h=h+deltah*Ts;

    if h<=0
        h=0;
    end
    if h>1.2
        h=1.2;
    end
    qut=z*Kc*sqrt(g*h);

    harray =[harray h];
    qin_array =[qin_array qinn];
    qout_array =[qout_array qut];
end


figure;
plot(harray,'LineWidth',1.1);
```

```
xlabel('Time [s]');
ylabel('Tank level [m]');
title('Tank level when changing flow
in','FontSize',16,'FontWeight','bold');
set(findall(gcf,'type','axes'),'fontsize',11);
grid on;
figure;
plot(1:Ts:Tf,qin_array,1:Ts:Tf,qout_array,'LineWidth',1.1);
xlabel('Time [s]');
ylabel('Flow rate [m3/s]');
title('Flow rate','FontSize',16,'FontWeight','bold');
set(findall(gcf,'type','axes'),'fontsize',11);
legend('Flow rate in (q in)','Flow rate out (q out)');
grid on;
```

10.2 Tank example with level control

```
clear all; clc;
close all;

Ts=1;
Ti=2.5;
Tf=2000;
qinn = 0.01666667;% [m3/s] (1000 l/min)
h=0.7;%[m]
A=10; %[ m]
rho=1620;
Kv=0.14;
g=9.81;
z=0.12;  %≈pning ut
delta_z=0;
e=0;
Kp=10.0;
Ki=0.85;
%Ki = Kp/Ti;
%Ki = 0.05;
%Ki = 999999999999;

qut=Kv*sqrt(g*h);


h_setp = 0.4;
h_setp_old = h_setp;

%min and max values
h_max = 1.2;
h_min = 0;
z_max = 1;
z_min = 0;
qinn_max = 0.04;
qinn_min = 0;


h_ar =[];
h_setp_ar =[];
z_ar =[];
y_ar =[];
u_ar =[];
ufb_ar =[];
uff_ar =[];
ufr_ar =[];

qinn_ar = [];
qut_ar = [];
zff_ar = [];
zfr_ar = [];

uff = 0;
ufr = 0;

for i=1:Ts:Tf

    %Update reference
    if (i > 500) && (i < (500)+60)
        h_setp = h_setp - 0.005;
    end
```

```
    %Update disturbance
    if (i >= 1000) && (i < (1000)+60)
      qinn = qinn+0.00027777833;% [m3/s] (ramp up to 2000 l/min in one
minute)
    end

    if (i >= 1500) && (i < (1500)+60)
      qinn = qinn-0.00027777833;% [m3/s] (ramp down to 1000 l/min in one
minute)
    end

    if i >= ((1500)+60)
      qinn = 0.01666667;% [m3/s] (2000 l/min)
    end

    % calculate z feed forward disturbance
    zff = qinn/(Kv*sqrt(g*h));
    %calculate z feed forward reference
    zfr = (A*(h_setp_old-h_setp))/(Kv*sqrt(g*h));
    h_setp_old = h_setp;
    %scale process variables to controller
    r = ((h_setp-h_min)/h_max)*100.0; % reference
    y = ((h-h_min)/h_max)*100.0; % controlled variable
    u = ((z-z_min)/z_max)*100.0; % manipulated variable
    uff_new = ((zff-z_min)/z_max)*100.0; % manipulated variable
    ufr_new = ((zfr-z_min)/z_max)*100.0; % manipulated variable
    %--
    %uff = 0; % turn off feedforward disturbance
    %ufr = 0; % turn off feedforward reference
    ufb = u-uff-ufr;
    %Store previous values
    last_e = e;
    e=y-r;
    %Controller
%    delta_u=Kp*(e-last_e)+((Kp*Ts)/Ti)*e;
    delta_u=Kp*(e-last_e)+(Ki*Ts)*e;
    ufb=ufb+delta_u;
    %ut=0;
    uff = uff_new; % comment update if ff dist is off
    ufr = ufr_new; % comment update if ff ref is off
    u = ufb +uff + ufr; %( feedback + ff dist + ff ref)
    if u<=0
        u=0;
    end
    if u>100
        u=100;
    end
    %--

    %scale controller variables to process
    z = z_min + z_max*(u/100.0);
    %--

    %simulere med ny regulatorsetting (z)
    qut=z*Kv*sqrt(g*h);
    deltah=(1/A)*(qinn*Ts-qut*Ts);
    h=h+deltah;
    % verify min,max levels in tank
    if h<=0
        h=0;
    end
```

```
    if h>2
        h=2;
    end


    %store to arrays
    h_ar =[h_ar h];
    h_setp_ar = [h_setp_ar h_setp];
    z_ar =[z_ar z];
    zff_ar = [zff_ar zff];
    zfr_ar = [zfr_ar zfr];
    y_ar =[y_ar y];
    u_ar =[u_ar u];
    ufb_ar =[ufb_ar ufb];
    uff_ar =[uff_ar uff];
    ufr_ar =[ufr_ar ufr];
    qinn_ar =[qinn_ar qinn];
    qut_ar =[qut_ar qut];

end
figure;
plot(1:Ts:Tf,h_ar,'b',1:Ts:Tf,h_setp_ar,'r','LineWidth',1.1);
legend('Actual','Reference');
xlabel('Time [s]');
ylabel('Tank level [m]');
title('Tank level with PI Controller','FontSize',16,'FontWeight','bold');
set(findall(gcf,'type','axes'),'fontsize',11)
grid on;

figure;
plot(y_ar);
xlabel('Time [s]');
ylabel('Tank level [%]');
title('Tank level with PID Controller');
grid on;

figure;
plot(z_ar);
xlabel('Time [s]');
ylabel('Choke opning [0-1]');
title('Choke opening with PID Controller');
grid on;

figure;
plot(zff_ar);
xlabel('Time [s]');
ylabel('Feed forward  disturbance choke opning [0-1]');
title('Feed forward choke opening direct');
grid on;

figure;
plot(zfr_ar);
xlabel('Time [s]');
ylabel('Feed forward reference choke opning [0-1]');
title('Feed forward choke opening direct');
grid on;

figure;
plot(u_ar,'LineWidth',1.1);
xlabel('Time [s]');
ylabel('Choke opning [%]');
```

```
title('Choke opening with PI
Controller','FontSize',16,'FontWeight','bold');
set(findall(gcf,'type','axes'),'fontsize',11);
grid on;

figure;
plot(ufb_ar);
xlabel('Time [s]');
ylabel('Choke opning feedback only [%]');
title('Choke opening with PID Controller');
grid on;

figure;
plot(uff_ar);
xlabel('Time [s]');
ylabel('Choke opning ff dist only[%]');
title('Choke opening with PID Controller');
grid on;

figure;
plot(ufr_ar);
xlabel('Time [s]');
ylabel('Choke opning ff ref only[%]');
title('Choke opening with PID Controller');
grid on;

figure;
plot(1:Ts:Tf,qinn_ar,'b',1:Ts:Tf,qut_ar,'r','LineWidth',1.1);
legend('Flow rate in (q in)','Flow rate out (q out)');
xlabel('Time [s]');
ylabel('Flow rate [m3/s]');
title('Flow rate','FontSize',16,'FontWeight','bold');
set(findall(gcf,'type','axes'),'fontsize',11);
grid on;
```

10.3 Kaasa model for MPD

```
%% Example of solving the Kaasa model using Euler integration
%
% Differential equations of Kaasa model:
% p_pdot = (beta_d/V_d)*(q_p-q_c)
% q_bdot = 1/M((p_p-p_c)-(Fd+Fb+Fa)*q_b*q_b+(rho_d-rho_a)*g*h)
% p_cdot = (beta_a/V_a)*(q_b+q_res+q_bpp-q_c)
% q_c = z_c*k_c*sqrt(p_c/rho_a)
%
% Parameters and initial values
clear all; % deletes all variables
close all; % removes all plot windows

% Constants
maxtime = 2000; % seconds
dt = 0.001; % euler step time
Ts = 1;% loop time step

%Operator parameters
q_p = 2000/60000; % 2000 l/min
q_bpp =0/60000; % 800 l/min
%q_bpp = 800/60000; % 800 l/min
q_c = q_p + q_bpp; % 2800 l/min
z_c = 0.2; % choke opening
q_rb = q_c;

% Wellbore parameters
h = 2000;
beta_d =2e9;
beta_a =1e9;
V_d =17; % m3
V_a = 48; %m3
A_a = 30/h;
A_r = 0.01; % Riser area
M = 4.3e8;
Fd = 5e9;
Fb = 1e9;
Fa = 2e9;
rho_d = 1580;
rho_a = 1580;
g = 9.81;
k_c = 0.021;
rho_w= 1000;


% Define range

p_min=0*10^7; % p_p_m
p_max=5.0*10^7; % p_bhp_m
z_min=0;
z_max=0.20;

qrb_min=0;
qrb_max=10000/60000;

% reservoir parameters
p_pore = 3.05e7;
p_frac = 3.75e7;
ProdIndex = 0;%(100/60000)/5e5; % 100 l/min at delta p of 5 bar %
'permeability'
```

```
%Array initialization
p_p_ar = zeros(maxtime,1);
p_c_ar = zeros(maxtime,1);
p_b_ar = zeros(maxtime,1);
p_b_r_ar = zeros(maxtime,1);
q_b_ar = zeros(maxtime,1);
q_c_ar = zeros(maxtime,1);
q_p_ar = zeros(maxtime,1);
q_bpp_ar = zeros(maxtime,1);
q_res_ar = zeros(maxtime,1);
r_ar = zeros(maxtime,1);
u_ar = zeros(maxtime,1);
y_ar = zeros(maxtime,1);
ufd_ar = zeros(maxtime,1);
h_rb_ar = zeros(maxtime,1);
z_c_ar = zeros(maxtime,1);

% Initial values
p_p = 20e5;
p_c = 10e5;
q_b = 2000/60000;
p_b = p_p + rho_d*g*h;
p_rb = 0;
h_rb = 0; % Level between water and drilling fluid measured from rb pump
h_rb_max= 1000; %Total riser height
q_of= 0; %Mud over flow at top of well
q_fill=0; %water rate at top of well (in/out)

%reference value
p_c_r = 15e5;
p_b_r = 450e5;

%Initialize controller
e = 0;
u = 0;
ufd = 0;
ufr = 0;
ufb = 0;
y = 0;
r = 0;
Kp = 11.5;
Ki = 0.5;


% Main iteration loop showing how the driller adjust the topside pump rate
for time = 1:maxtime

    p_c_r_last = p_c_r;


%     if (time > 100) && (time <= 200)
%         q_p = q_p + 5/60000; % ramp up to 2500 l/min
%     end
%     if (time > 200) && (time <= 300)
%         q_p = 2500/60000; % fixed at 2500 l/min
%     end
%
%     if (time > 300) && (time <= 350)
%
%         q_p = q_p - 3/60000; % ramp down to 1000 l/min
```

```
%     end
%
%     if (time > 400)
%
%     end
%
%     if (time > 700) && (time <= 730)
%
%         q_p = q_p - 30/60000; % ramp down to 1000 l/min
%
%     end

 if (time > 200) && (time <= 200+60*2)
        q_p = q_p -1000/60000/60; % (ramp down by 1000 l/min in one minute)
    end

    if (time > 200+60*2) && (time <= 600)

        q_p = 0;
    end

    if (time > 600)&& (time <= 600+60*2)
        q_p = q_p +1000/60000/60; % (ramp up by 1000 l/min in one minute)
    end

    if (time > 600+60*2) && (time <= 1200)

        q_p = 2000/60000;

    end
    if (time > 1200) && (time <= 1200+60*2)
        q_p = q_p -1000/60000/60; % (ramp down by 1000 l/min in one minute)
    end

    if (time > 1200+60*2) && (time <= 1600)

        q_p = 0;
    end

    if (time > 1600)&& (time <= 1600+60*2)
        q_p = q_p +1000/60000/60; % (ramp up by 1000 l/min in one minute)
    end

    if (time > 1600+60*2)

        q_p = 2000/60000;

    end

    %Loop that can be used for lost circulation or influx
    %Pore pressure
    q_res = ProdIndex*(p_pore - p_b);

    if q_res < 0
        q_res = 0;
    end

    % Frac pressure
    q_loss = ProdIndex*(p_frac -p_b);
    if q_loss > 0
```

```
        q_loss = 0;
    end


    %store parameters
    p_p_ar(time) = p_p;
    p_c_ar(time) = p_c;
    p_c_r_ar(time) = p_c_r;
    p_b_r_ar(time) = p_b_r;
    p_b_ar(time) = p_b;
    q_b_ar(time) = q_b;
    q_p_ar(time) = q_p;
    q_c_ar(time) = q_c;
    q_bpp_ar(time) = q_bpp;
    q_res_ar(time) = q_res;
    q_rb_ar(time) = q_rb;
    u_ar(time) = u;
    y_ar(time) = y;
    r_ar(time) = r;
    ufd_ar(time) = ufd;
    ufr_ar(time) = ufr;
    h_rb_ar(time) = h_rb;
    q_of_ar(time) = q_of;
    q_fill_ar(time) = q_fill;
    z_c_ar(time) = z_c;



    %% Controller code

    % Feed forward from disturbance
    zfr = ((V_a/beta_a)*(p_c_r_last-p_c_r))/(k_c*sqrt(p_c/rho_a));

    zfd = (q_p + q_bpp)/(k_c*sqrt(p_c/rho_a));



    % scale to percentace
    r = ((p_b_r-p_min)/p_max)*100.0; % reference is p_b1
    y = ((p_b-p_min)/p_max)*100.0; % controlled variable
    u = ((q_rb-qrb_min)/qrb_max)*100.0; % manipulated variable
 %   ufd_last = ufd;
    ufd = ((zfd-z_min)/z_max)*100.0; % feed forward disturbance
    ufr = ((zfr-z_min)/z_max)*100.0; % feed forward disturbance
    %ufb = u ;b1

    % controller code
    last_e = e;
    e=y-r;
%    delta_u=Kp*(e-last_e)+((Kp*Ts)/Ti)*e; % using Kp and Ti
    delta_u=Kp*(e-last_e)+(Ki*Ts)*e; % using Kp and Ki


    ufb=ufb+delta_u; % feedback


    u = ufb; % +ufd+ufr;
%    u = ufb+ufd_last; % +ufd+ufr; with time delay
%    u = ufb+ufd; % +ufd+ufr;
    u = ufb+ufd+ufr; % +ufd+ufr;
```

```
    %limit p_c
    if p_c<0
       p_c=0;
    end

    % limit u
    if u<=0
       u=0;
    end

    if u>100
        u=100;
    end


    %scale to physical values (only z are needed
    z_c_old = z_c;
    z_c = z_min + z_max*(u/100.0);
    %z_c=0.1;




    % Euler integration loop
    for eulerstep = 1:(1/dt)
        p_pdot = (beta_d/V_d)*(q_p-q_b);
        q_bdot = 1/M*((p_p-(p_c))-(Fd+Fb+Fa)*q_b*q_b+(rho_d-rho_a)*g*h);
        p_cdot = (beta_a/V_a)*(q_b+q_res+q_bpp+q_loss-q_c);



        p_p = p_p + p_pdot*dt;
        q_b = q_b + q_bdot*dt;
        p_c = p_c + p_cdot*dt;


        q_c = z_c*k_c*sqrt(p_c/rho_a);
        p_b1  = p_p+rho_d*g*h-(Fd+Fb)*q_b*q_b; % pump pressure
        p_b =p_rb*0+p_c+rho_a*g*h+Fa*q_b*q_b; % using choke pressure

    end
end

% figure(1);
% plot(1:maxtime,p_b_ar,'b','LineWidth',1.1);
% legend('Downhole pressure [Pa]');hold on
% axis([200,700,4.4*10^7,4.6*10^7])
% grid

figure(1);
plot(1:maxtime,p_b_ar,'b',1:maxtime,p_b_r_ar,'--k','LineWidth',1.1);
xlabel('Time [s]','fontsize',14);
legend('Measured','Reference');hold on
title('Downhole pressure [Pa]','FontSize',16,'FontWeight','bold');
set(findall(gcf,'type','axes'),'fontsize',11)
%axis([0,2000,3*10^7,4.6*10^7])
grid
```

```
figure;
plot(1:maxtime,p_p_ar,'b','LineWidth',1.1);
legend('Measured');
title('Pump pressure [Pa]');
%axis([0,2000,-2*10^7,2*10^7])
grid

% figure
% plot(1:maxtime,p_c_ar,'b',1:maxtime,p_c_r_ar,'k');
% legend('Measured','Reference');
% title('Choke pressure [Pa]');
% grid

figure
plot(1:maxtime,p_c_ar,'b','LineWidth',1.1);
xlabel('Time [s]','fontsize',14);
legend('Measured','Reference');
title('Choke pressure [Pa]','FontSize',16,'FontWeight','bold');
set(findall(gcf,'type','axes'),'fontsize',11)
%axis([0,2000,-0.02*10^7,0.12*10^7])
grid

figure;
plot(1:maxtime,q_b_ar*60000,'b',1:maxtime,q_p_ar*60000,'g',...
    1:maxtime,q_bpp_ar*60000,'k',1:maxtime,q_c_ar*60000,'r',...
    1:maxtime,q_res_ar*60000,'c', 1:maxtime,q_rb_ar*60000,'m');
title('Flow rate [l/min]');
legend('bit','rigpump','backpp','choke','res','riser');
grid

%figure;
%plot(1:maxtime,r_ar,'k',1:maxtime,y_ar,'g',1:maxtime,u_ar,'b',1:maxtime,uf
d_ar,'r',1:maxtime,ufr_ar,'c');
%legend('Reference (r)','Controlled Variable (y)','Manipulated variable
(u)',...
    %'Feedforward dist (ufb)','Feedforward ref (ufr)');
%axis([1 maxtime 0 100]);
%title('Controller values');
%grid

figure;
plot(1:maxtime,p_b_ar,'b',1:maxtime,rho_a*g*(h+h_rb_ar),'r',1:maxtime,p_b_a
r-(rho_a*g*(h+h_rb_ar)),'g');
title('Downhole pressure [Pa]');
legend('ECD','Hydrostatic Part','Frictional Part')
grid

% figure;
% plot(1:maxtime,rho_a*g*(h_rb_ar),'r',1:maxtime,p_b_ar-
(rho_a*g*(h+h_rb_ar)),'g');
% title('Downhole pressure [Pa]');
% legend('Hydrostatic pressure@Riserbase','Fricational Pressure Drop')

figure;
plot(1:maxtime,q_p_ar*60000,'b','LineWidth',1.1);
xlabel('Time [s]','fontsize',14);
title('Flowrate in [l/min]','FontSize',16,'FontWeight','bold');
set(findall(gcf,'type','axes'),'fontsize',11)
%axis([0,2000,-0.02*10^7,0.12*10^7])
legend('Rigpump');
```

```
figure;
plot(1:maxtime,z_c_ar,'LineWidth',1.1);
xlabel('Time [s]','fontsize',14);
ylabel('Choke opening [0-1]','fontsize',14);
title('Choke opening with PI
Controller','FontSize',16,'FontWeight','bold');
set(findall(gcf,'type','axes'),'fontsize',11)
axis([0,2000,0,0.2])
grid on;

figure;
plot(1:maxtime,z_c_ar,'LineWidth',1.1);
xlabel('Time [s]','fontsize',14);
ylabel('Choke opening [0-1]','fontsize',14);
title('Constant choke opening','FontSize',16,'FontWeight','bold');
set(findall(gcf,'type','axes'),'fontsize',11)
axis([0,2000,0,0.2])
grid on;
```

10.4 Kaasa model for DGD

```
%% Example of solving the Kaasa model using Euler integration
%
% Differential equations of Kaasa model:
% p_pdot = (beta_d/V_d)*(q_p-q_c)
% q_bdot = 1/M((p_p-(p_c+p_rb))-(Fd+Fb+Fa)*q_b*q_b+(rho_d-rho_a)*g*h)
% p_cdot = (beta_a/V_a)*(q_b+q_res+q_bpp-q_c)
% q_c = z_c*k_c*sqrt(p_c/rho_a)
%
% Parameters and initial values
clear all; % deletes all variables
 close all; % removes all plot windows

% Constants
maxtime = 2000; % seconds
dt = 0.01; % euler step time
Ts = 1;% loop time step

%Operator parameters
q_p = 2000/60000; % 2000 l/min
q_bpp =0/60000; % 800 l/min
%q_bpp = 800/60000; % 800 l/min
q_c = q_p + q_bpp; % 2800 l/min
z_c = 0.2; % choke opening

q_top=2000/60000;
%q_top=4000/60000; % Increased topfill flowrate
%q_top=1000/60000; % Lowered topfill flowrate
q_rb = q_c+q_top;
% Wellbore parameters
h = 2000;
beta_d =2e9;
beta_a =1e9;
V_d =17; % m3
V_a = 48; %m3
A_a = 30/h;
A_r = 0.01; % Riser area
M = 4.3e8;
Fd = 5e9;
Fb = 1e9;
Fa = 2e9;
rho_d = 1580;
rho_a = 1580;
g = 9.81;
k_c = 0.021;
rho_w=1000;
%rho_w= 1100; % Increased topfill fluid density
%rho_w= 800; % Lowered topfill fluid density

h_rb = 600; % Level between water and drilling fluid measured from rb pump
%h_rb = 300; % Level between water and drilling fluid measured from rb pump
(increased total riser height)
%h_rb_max= 1000; %Total riser height
%h_rb_max= 1100; %Increased total riser height
h_rb_max= 900; %Lowered total riser height



% Define range
```

```
p_min=0*10^7; % p_p_m
p_max=5.0*10^7; % p_bhp_m
z_min=0;
z_max=0.20;

qrb_min=0;
qrb_max=10000/60000;

% reservoir parameters
p_pore = 3.05e7;
p_frac = 3.75e7;
ProdIndex = 0;%(100/60000)/5e5; % 100 l/min at delta p of 5 bar %
'permeability'

%Array initialization
p_p_ar = zeros(maxtime,1);
p_c_ar = zeros(maxtime,1);
p_b_r_ar = zeros(maxtime,1);
p_b_ar = zeros(maxtime,1);
q_b_ar = zeros(maxtime,1);
q_c_ar = zeros(maxtime,1);
q_p_ar = zeros(maxtime,1);
q_bpp_ar = zeros(maxtime,1);
q_res_ar = zeros(maxtime,1);
r_ar = zeros(maxtime,1);
u_ar = zeros(maxtime,1);
y_ar = zeros(maxtime,1);
ufd_ar = zeros(maxtime,1);
h_rb_ar = zeros(maxtime,1);
q_top_ar = zeros(maxtime,1);

% Initial values
p_p = 20e5;
p_c = 10e5;
q_b = 2000/60000;
p_b = p_p + rho_d*g*h;
p_rb = 0;
q_of= 0; %Mud over flow at top of well
q_fill=0; %water rate at top of well (in/out)

%reference value
p_c_r = 15e5;
p_b_r = 450e5;

%Initialize controller
e = 0;
u = 0;
ufd = 0;
ufr = 0;
ufb = 0;
y = 0;
r = 0;
%Kp = 80;
%Ki = 0.2;

Kp = 65; % For lowered topfill fluid density
Ki = 0.3; % For lowered topfill fluid density


% Main iteration loop showing how the driller adjust the topside pump rate
for time = 1:maxtime
```

```
    p_b_r_last = p_b_r;


%     if (time > 100) && (time <= 200)
%         q_p = q_p + 5/60000; % ramp up to 2500 l/min
%     end
%     if (time > 200) && (time <= 300)
%         q_p = 2500/60000; % fixed at 2500 l/min
%     end
%
%     if (time > 300) && (time <= 350)
%
%         q_p = q_p - 3/60000; % ramp down to 1000 l/min
%     end
%
%     if (time > 400)
%
%     end
%
%     if (time > 700) && (time <= 730)
%
%         q_p = q_p - 30/60000; % ramp down to 1000 l/min
%
%     end

     if (time > 200) && (time <= 200+60*2)
        q_p = q_p -1000/60000/60; % (ramp down by 1000 l/min in one minute)
    end

    if (time > 200+60*2) && (time <= 600)

        q_p = 0;
    end

    if (time > 600)&& (time <= 600+60*2)
        q_p = q_p +1000/60000/60; % (ramp up by 1000 l/min in one minute)
    end

    if (time > 600+60*2) && (time <= 1200)

        q_p = 2000/60000;

    end
    if (time > 1200) && (time <= 1200+60*2)
        q_p = q_p -1000/60000/60; % (ramp down by 1000 l/min in one minute)
    end

    if (time > 1200+60*2) && (time <= 1600)

        q_p = 0;
    end

    if (time > 1600)&& (time <= 1600+60*2)
        q_p = q_p +1000/60000/60; % (ramp up by 1000 l/min in one minute)
    end

    if (time > 1600+60*2)

        q_p = 2000/60000;
```

```
    end

    %Loop that can be used for lost circulation or influx
    %Pore pressure
    q_res = ProdIndex*(p_pore - p_b);

    if q_res < 0
        q_res = 0;
    end

    % Frac pressure
    q_loss = ProdIndex*(p_frac -p_b);
    if q_loss > 0
        q_loss = 0;
    end


    %store parameters
    p_p_ar(time) = p_p;
    p_c_ar(time) = p_c;
    p_c_r_ar(time) = p_c_r;
    p_b_ar(time) = p_b;
    p_b_r_ar(time) = p_b_r;
    q_b_ar(time) = q_b;
    q_p_ar(time) = q_p;
    q_c_ar(time) = q_c;
    q_bpp_ar(time) = q_bpp;
    q_res_ar(time) = q_res;
    q_rb_ar(time) = q_rb;
    u_ar(time) = u;
    y_ar(time) = y;
    r_ar(time) = r;
    ufd_ar(time) = ufd;
    ufr_ar(time) = ufr;
    h_rb_ar(time) = h_rb;
    q_of_ar(time) = q_of;
    q_fill_ar(time) = q_fill;
    q_top_ar(time) = q_top;



    %% Controller code

    % Feed forward from disturbance
    zfr = (V_a/beta_a)*(p_b_r_last-p_b_r);

    zfd = (q_p + q_bpp);



    % scale to percentace
    r = ((p_b_r-p_min)/p_max)*100.0; % reference is p_b1
    y = ((p_b-p_min)/p_max)*100.0; % controlled variable
    u = ((q_rb-qrb_min)/qrb_max)*100.0; % manipulated variable
%   ufd_last = ufd;
    ufd = ((zfd-z_min)/z_max)*100.0; % feed forward disturbance
    ufr = ((zfr-z_min)/z_max)*100.0; % feed forward disturbance
    %ufb = u ;b1
```

```
    % controller code
    last_e = e;
    e=y-r;
%    delta_u=Kp*(e-last_e)+((Kp*Ts)/Ti)*e; % using Kp and Ti
    delta_u=Kp*(e-last_e)+(Ki*Ts)*e; % using Kp and Ki


    ufb=ufb+delta_u; % feedback


    u = ufb; % +ufd+ufr;
%    u = ufb+ufd_last; % +ufd+ufr; with time delay
%    u = ufb+ufd; % +ufd+ufr;
     u = ufb+ufd+ufr; % +ufd+ufr;

    % limit u
    if u<=0
       u=0;
    end

    if u>100
        u=100;
    end



    %scale to physical values (only z are needed
%      z_c_old = z_c;
%      z_c = z_min + z_max*(u/100.0);
    q_rb_old = q_rb;
    q_rb = qrb_min + (qrb_max-qrb_min)*(u/100.0);

    %



    % Euler integration loop
    for eulerstep = 1:(1/dt)
        p_pdot = (beta_d/V_d)*(q_p-q_b);
        q_bdot = 1/M*((p_p-(p_c+p_rb))-(Fd+Fb+Fa)*q_b*q_b+(rho_d-
rho_a)*g*h);
        p_cdot = (beta_a/V_a)*(q_b+q_res+q_bpp+q_loss-q_c);

        if h_rb < h_rb_max
          h_rbdot = (1/A_r)*(q_c+q_top-q_rb);
          q_of=0;
          q_fill= -q_c+q_rb-q_top;
        else
            h_rbdot = 0;
            q_of = (q_c-q_rb);
            q_fill=0;
        end



        p_p = p_p + p_pdot*dt;
        q_b = q_b + q_bdot*dt;
        p_c = p_c + p_cdot*dt;
        h_rb = h_rb + h_rbdot*dt;

        if p_c<0
```

```
            q_c=0;
        else
            q_c = z_c*k_c*sqrt(p_c/rho_a);
            p_rb = rho_a*g*h_rb+ rho_w*g*(h_rb_max-h_rb);
            p_b1  = p_p+rho_d*g*h-(Fd+Fb)*q_b*q_b; % pump pressure
            p_b =p_rb+p_c+rho_a*g*h+Fa*q_b*q_b; % using choke pressure
      end



    end
end

figure;
plot(1:maxtime,p_b_ar,'b',1:maxtime,p_b_r_ar,'--k','LineWidth',1.1);
xlabel('Time [s]','fontsize',14);
legend('Measured','Reference');
title('Downhole pressure [Pa]','FontSize',16,'FontWeight','bold');
set(findall(gcf,'type','axes'),'fontsize',11)
grid
axis([0,2000,4.4*10^7,4.85*10^7])
%axis([0,2000,4.4*10^7,5.19*10^7])

figure;
plot(1:maxtime,p_p_ar,'b','LineWidth',1.1);
title('Pump pressure [Pa]');
grid

figure;
plot(1:maxtime,p_c_ar,'b',1:maxtime,p_c_r_ar,'k','LineWidth',1.1);
legend('Measured','Reference');
title('Choke pressure [Pa]');
grid

% figure;
% plot(1:maxtime,q_b_ar*60000,'b',1:maxtime,q_p_ar*60000,'g',...
%     1:maxtime,q_bpp_ar*60000,'k',1:maxtime,q_c_ar*60000,'r',...
%     1:maxtime,q_res_ar*60000,'c', 1:maxtime,q_rb_ar*60000,'m');
% title('Flow rate [l/min]');
% legend('bit','rigpump','backpp','choke','res','riser');
% grid

figure;
plot(1:maxtime,q_b_ar*60000,'m',1:maxtime,q_c_ar*60000,'r',...
    1:maxtime,q_res_ar*60000,'c',1:maxtime,q_rb_ar*60000,'b',...
    1:maxtime,q_top_ar*60000,'--k','LineWidth',1.1);
xlabel('Time [s]','fontsize',14);
title('Flow rate [l/min]','FontSize',16,'FontWeight','bold');
set(findall(gcf,'type','axes'),'fontsize',11)
legend('Bit','Choke','Reservoir','Subsea pump','Topfill pump');
grid

%figure;
%plot(1:maxtime,r_ar,'k',1:maxtime,y_ar,'g',1:maxtime,u_ar,'b',1:maxtime,uf
d_ar,'r',1:maxtime,ufr_ar,'c');
%legend('Reference (r)','Controlled Variable (y)','Manipulated variable
(u)',...
%    'Feedforward dist (ufb)','Feedforward ref (ufr)');
%axis([1 maxtime 0 100]);
%title('Controller values');
%grid
```

```
figure;
plot(1:maxtime,h_rb_ar,'b','LineWidth',1.1);
xlabel('Time [s]','fontsize',14);
title('Riser level [m]','FontSize',16,'FontWeight','bold');
set(findall(gcf,'type','axes'),'fontsize',11)
grid
%
% figure;
%
plot(1:maxtime,p_b_ar,'b',1:maxtime,rho_a*g*(h+h_rb_ar),'r',1:maxtime,p_b_a
r-(rho_a*g*(h+h_rb_ar)),'g');
% title('Downhole pressure [Pa]');
% legend('ECD','Hydrostatic Part','Frictional Part')
%
% figure;
% plot(1:maxtime,rho_a*g*(h_rb_ar),'r',1:maxtime,p_b_ar-
(rho_a*g*(h+h_rb_ar)),'g');
% title('Downhole pressure [Pa]');
% legend('Hydrostatic pressure@Riserbase','Fricational Pressure Drop')
%
 figure;
 plot(1:maxtime,q_p_ar*60000,'b','LineWidth',1.1);
 xlabel('Time [s]','fontsize',14);
 title('Flowrate in [l/min]','FontSize',16,'FontWeight','bold');
 set(findall(gcf,'type','axes'),'fontsize',11)
 legend('Rigpump');
%
% figure;
% plot(1:maxtime,q_of_ar*60000,'b');
% title('Lost overflow [l/min]');
% legend('Overflow of drilling fluid');
%
% figure;
%  plot(1:maxtime,q_fill_ar*60000,'g','LineWidth',1.1);
%  title('Water fill at top [l/min]');
%  legend('Water fill at top');
```